Openventio PUBLISHERS

ISSN 2475-1278

THE OPHTHALMOLOGY OPEN JOURNAL

| February 2017 | Volume 2 | Issue 1 |

www.openventio.org

THE OPHTHALMOLOGY OPEN JOURNAL

Openventio PUBLISHERS

ISSN 2475-1278

TABLE OF CONTENTS

THE OPHTHALMOLOGY OPEN JOURNAL

Openventio PUBLISHERS

ISSN 2475-1278 http://dx.doi.org/10.17140/OOJ-2-e004

Editorial

Corresponding author
Raúl Martín, OD (EC), MSc, PhD
Optometry Research Group
IOBA Eye Institute
University of Valladolid
Valladolid 47002, Spain;
School of Health Professions
Plymouth University
Plymouth PL4 8AA, UK
Tel. 983 184848
E-mail: raul@ioba.med.uva.es

Volume 2 : Issue 1
Article Ref. #: 1000OOJ2e004

Article History
Received: August 15th, 2016
Accepted: August 16th, 2016
Published: August 17th, 2016

Citation
Ortiz-Toquero S, Martin R. Fitting gas permeable contact lens in keratoconus, still a challenge? *Ophthalmol Open J.* 2016; 2(1): e1-e4. doi: 10.17140/OOJ-2-e004

Fitting Gas Permeable Contact Lens in Keratoconus; Still a Challenge?

Sara Ortiz-Toquero, OD (EC), MSc[1]; Raúl Martín, OD (EC), MSc, PhD[1,2*]

[1]Optometry Research Group, IOBA Eye Institute and Departamento de Física Teórica, Atómica y Óptica, University of Valladolid, Valladolid 47002, Spain
[2]School of Health Professions, Plymouth University, Plymouth PL4 8AA, UK

Gas permeable (GP) contact lenses (CL) are of paramount importance in keratoconus patient management[1] to rehabilitate vision and improve patients' quality of life (QoL).[2] Different surgical and non-surgical options are available in keratoconus management. Early stages could be managed with conventional optical corrections (spectacles and/or soft CL), however if disease progress, and corneal irregularity affects to visual acuity GP (conventional or with keratoconus specific design) lenses should be necessaries to patients' visual rehabilitation. Other alternative CL options (piggy-back, mini-scleral, semi-scleral, scleral designs etc.) have been, also, proposed. If patients show CL intolerance or disease progresses and/or corneal integrity could be affected surgical techniques are required.

Keratoconus diagnosis and management is a challenge. The first difficulty is related with an accurate identification of keratoconus patient.[1] Clear diagnosis of early stage (in opposition to moderate or advanced disease), subclinical keratoconus, or how distinguish keratoconus from other ectatic diseases imposes greater diagnostic challenges.[1,3] A complete eye exam is necessary to confirm keratoconus diagnosis, make the differential diagnosis with subclinical keratoconus and differentiate of other ectatic diseases. Anterior eye investigation; based on slit lamp findings (stromal thinning, conical protrusion, Fleischer ring and Vogt striae); corneal tomography (Scheimpflug or optical coherence tomography) assessing anterior and posterior corneal surface; and full corneal thickness map analysis (because normal central thickness could be present in keratoconus cornea) are mandatory. Anterior topographical analysis (Placido-based topographers) still plays a relevant role in keratoconus detection, especially in primary care, because these devices are one of the most extensively used in clinical practice[4,5] and aid to differentiate between keratoconus and pellucid marginal degeneration (PMD).[1] Patients' history may identify major risk factors for keratoconus; such as: down syndrome, relatives of affected patients, ocular allergy, Asian or Arabian ethnicity, eye rubbing, floppy eyelid syndrome, atopy, connective tissue disorders (Marfan syndrome), and others.[1,6]

The second challenge is related with disease classification because there is no clinically adequate classification system for keratoconus disease.[1] Amsler-Krumeich classification[7,8] and collaborative longitudinal evaluation of keratoconus (CLEK)[9] classifications are the most commonly used to classify the keratoconus severity. Amsler-Krumeich classification proposes four different levels using refractive, topographic and biomicroscopic corneal signs. The CLEK classification[9] proposes to use the average corneal power and root mean square (RMS) error for higher-order Zernike terms (derived from the first corneal surface wavefront) combined with clinical biomicroscopic signs. However, both classifications fail to address current information and technological advances[1] and a new classification criterion is necessary. Although, there is a lack of consensus in this issue, high order corneal aberration analysis could play a relevant role in future keratoconus classification[3] because larger values of vertical coma has been founded in these patients.[4,9-11] Clinical progression requires changes in at least 2 of these 3 parameters; corneal steepening (anterior and/or posterior) and progressive corneal thinning.[1] That means that disease progression is directly dependent of the accuracy and reliability of the corneal device used in patient assessment.[5,10]

ISSN 2475-1278 http://dx.doi.org/10.17140/OOJ-2-e004

After diagnosis and gradation of the keratoconus disease, management and treatment could be the third challenge. Two major approaches; surgical and non-surgical management have been proposed, with the objective of halt progression of the disease and patients' visual rehabilitation. Non-surgical approach may be the first action in patient management (less invasive therapeutic strategies), highlighting GP CL fitting to improve patients' vision, although GP CL wear do not halt the progression of the disease.[12] Patient education avoiding eye rubbing is, also, necessary.[1,6]

Different surgical options are currently available without clear consensus regarding what could be the best surgical approach for keratoconus. Corneal cross-linking (CXL) has been proposed in patients younger than 40 years to halt disease progression with limited evidence provided by properly conducted randomized controlled trial (RCT)[13] and requires a well-documented clinical progression or risk of progression patient. It is, also, unclear it uses in subclinical keratoconus patients.[1] Light improvement of visual acuity (1 to 2 Snellen lines) could be expected after CXL.[14] Descemetic deep anterior lamellar (dDALK), in patients without Descemet membrane compromise, or penetrating keratoplasty (PK) are the "techniques of choice" when a corneal transplant was needed (in advance disease stages; severe corneal thinning; or in non-CL tolerant patients). These techniques achieved best-corrected visual acuity of 20/40 or better in 3 of 4 patients,[15] with insufficient evidence to determine which technique offer better overall outcomes.[16] Intracorneal ring segment (ICRS) increases corneal stability decreasing the astigmatism asymmetry helping in normalization of the corneal contour with slight improvement of patients' visual acuity,[12,17] without clear consensus about its indication.

Notwithstanding, if patient is satisfied with their vision (with spectacles or CL) no surgical treatment is indicated (except CXL), so visual rehabilitation of keratoconus patient is of paramount importance.[1] Although GP CL raises keratoconus patients' visual acuity (VA) near to 20/20,[18] achieve the correct lens parameters is a challenge to practitioners and patients[19] requiring several diagnostic lenses to achieve a final acceptable GP lens fit, which prolongs practitioner and patient chair time. To improve CL fitting procedure, different CL design and strategies have been proposed. For example, the use of CL fitting software linked with different corneal topographers could help in GP lens fitting[20,21] but, a lack in clinical studies that analyze the real impact of these software in clinical practice exists. Some of these software propose GP lens with systematic bias that could be improve with new equations.[22]

Recently, a new clinically validated open access web-calculator (www.calculens.com) has been developed with the aim to aid CL practitioners to calculate CL parameters of the GP lens to be fitted in keratoconus patients (European Academy of Optic and Optometry 2016 Meeting). This new tool will allow that keratoconus patients receive the most adequate lens and help CL practitioners to provide a sound fitting process, decreasing the number of diagnostic lenses, trials, and chair time to those achieved in standard GP CL fitting.[23] Therefore with this new tool, keratoconus management with GP CL will be not a challenge any more; and both, patients and practitioners, will be benefited.

In conclusion, Keratoconus is a multifactorial disease with genetic, biochemical, biomechanical, and environmental pathophysiology[1]; that requires a multiprofessional approach for early detection, correct diagnosis, follow-up, monitoring and adequate patient management that involve; primary eye care practitioners, optometrists, CL practitioners and ophthalmologists with the last aim to provide better care and improve patients' quality of life.

CONFLICTS OF INTEREST

The authors declare that they have no conflicts of interest.

REFERENCES

1. Gomes JA, Tan D, Rapuano CJ, et al. Global consensus on keratoconus and ectatic diseases. *Cornea*. 2015; 34: 359-369. doi: 10.1097/ICO.0000000000000408

2. Ortiz-Toquero S, Perez S, De Juan V, Rodriguez G, Agustin Mayo-Iscar A, Martin R. The influence of the refractive correction on the vision-related quality of life in keratoconus patients. *Qual Life Res*. 2015; 25(4): 1043-1051. doi: 10.1007/s11136-015-1117-1

3. Sideroudi H, Labiris G, Georgatzoglou K, Ditzel F, Siganos C, Kozobolis V. Fourier analysis of videokeratography data: Clinical usefulness in grade I and subclinical keratoconus. *J Cataract Refract Surg*. 2016; 42: 731-737. doi: 10.1016/j.jcrs.2016.01.049

4. Piñero DP, Nieto JC, Lopez-Miguel A. Characterization of corneal structure in keratoconus. *J Cataract Refract Surg*. 2012; 38: 2167-2183. doi: 10.1016/j.jcrs.2012.10.022

ISSN 2475-1278 http://dx.doi.org/10.17140/OOJ-2-e004

5. Ortiz-Toquero S, Rodriguez G, de Juan V, Martin R. Repeatability of placido-based corneal topography in keratoconus. *Optom Vis Sci.* 2014; 91(12): 1467-1473. doi: 10.1097/OPX.0000000000000421

6. Gordon-Shaag A, Millodot M, Shneor E, Liu Y. The genetic and environmental factors for keratoconus. *Biomed Res Int.* 2015; 2015: 795738. doi: 10.1155/2015/795738

7. Amsler M. Kératocõne classique et kératocône fruste; arguments unitaires [In French]. *Ophthalmologica*. 1946; 111: 96-101.

8. Krumeich JH, Daniel J, Knülle A. Live-epikeratophakia for keratoconus. *J Cataract Refract Surg.* 1998; 24: 456-463. doi: 10.1016/S0886-3350(98)80284-8

9. McMahon TT, Szczotka-Flynn L, Barr JT, et al. A new method for grading the severity of keratoconus: The Keratoconus Severity Score (KSS). *Cornea.* 2006; 25(7): 794-800. Web site. https://vrcc.wustl.edu/clekarchive/pdf/31%20McMahon%20-%20A%20New%20Method.pdf. Accessed August 14, 2016

10. Ortiz-Toquero S, Rodriguez G, de Juan V, Martin R. Repeatability of wavefront aberration measurements with a placido-based topographer in normal and keratoconic eyes. *J Refract Surg.* 2016; 32: 338-344. doi: 10.3928/1081597X-20160121-04

11. Alió JL, Shabayek MH. Corneal higher order aberrations: A method to grade keratoconus. *J Refract Surg.* 2006; 22: 539-545. doi: 10.3928/1081-597X-20060601-05

12. Mandathara PS, Stapleton FJ, Willcox MD. Outcome of keratoconus management: Review of the past 20 years' contemporary treatment modalities. *Eye Contact Lens*. 2016; 11. doi: 10.1097/ICL.0000000000000270

13. Sykakis E, Karim R, Evans JR, et al. Corneal collagen cross-linking for treating keratoconus. *Cochrane Database Syst Rev*. 2015; 24: CD010621. doi: 10.1002/14651858.CD010621.pub2

14. Meiri Z, Keren S, Rosenblatt A, Sarig T, Shenhav L, Varssano D. Efficacy of corneal collagen cross-linking for the treatment of Keratoconus: A systematic review and meta-analysis. *Cornea.* 2016; 35: 417-428. doi: 10.1097/ICO.0000000000000723

15. Arnalich-Montiel F, Alió del Barrio JL, Alió JL. Corneal surgery in keratoconus: Which type, which technique, which outcomes? *Eye Vis (Lond)*. 2016; 3: 2. doi: 10.1186/s40662-016-0033-y

16. Keane M, Coster D, Ziaei M, Williams K. Deep anterior lamellar keratoplasty versus penetrating keratoplasty for treating keratoconus. *Cochrane Database Syst Rev*. 2014; 22: CD009700. doi: 10.1002/14651858.CD009700.pub2

17. Poulsen DM, Kang JJ. Recent advances in the treatment of corneal ectasia with intrastromal corneal ring segments. *Curr Opin Ophthalmol*. 2015; 26: 273-277. doi: 10.1097/ICU.0000000000000163

18. Visser ES, Wisse RP, Soeters N, Imhof SM, Van der Lelij A. Objective and subjective evaluation of the performance of medical contact lenses fitted using a contact lens selection algorithm. *Cont Lens Anterior Eye.* 2016; 39(4): 298-306. doi: 10.1016/j.clae.2016.02.006

19. Zhou AJ, Kitamura K, Weissman BA. Contact lens care in keratoconus. *Cont Lens Anterior Eye.* 2003; 26: 171-174. doi: 10.1016/S1367-0484(03)00042-0

20. Mandathara PS, Fatima M, Taureen S, et al. GP contact lens fitting in keratoconus using FITSCAN technology. *Cont Lens Anterior Eye.* 2013; 36: 126-129. doi: 10.1016/j.clae.2012.12.002

21. Nosch DS, Ong GL, Mavrikakis I, et al. The application of a computerised videokeratography (CVK) based contact lens fitting software programme on irregularly shaped corneal surfaces. *Cont Lens Anterior Eye*. 2007; 30: 239-248. doi: 10.1016/j.clae.2007.06.003

22. Ortiz-Toquero S, Rodriguez G, De Juan V, Martin R. Rigid gas permeable contact lens fitting using new software in keratoconic eyes. *Optom Vis Sci.* 2016; 93: 286-292. doi: 10.1097/OPX.0000000000000804

ISSN 2475-1278 http://dx.doi.org/10.17140/OOJ-2-e004

23. Ortiz-Toquero S, Martin M, Rodriguez G, De Juan V, Martin R. Success of rigid gas permeable contact lens fitting. *Eye Contact Lens*. 2016; 13. doi: 10.1097/ICL.0000000000000254

THE OPHTHALMOLOGY OPEN JOURNAL

Openventio PUBLISHERS

ISSN 2475-1278 http://dx.doi.org/10.17140/OOJ-2-e005

Editorial

*Corresponding author
Digvijay Singh, FAICO, MD, MBBS
Consultant
Division of Ophthalmology
Medanta-The Medicity
Gurgaon, Haryana 122001, India
Tel. +91-9811664647
E-mail: drsingh.digvijay@gmail.com

Volume 2 : Issue 1
Article Ref. #: 1000OOJ2e005

Article History
Received: August 31st, 2016
Accepted: August 31st, 2016
Published: September 12th, 2016

Citation
Singh D. Automated image analysis software: Valuable tools for the future. *Ophthalmol Open J*. 2016; 2(1): e5-e6. doi: 10.17140/OOJ-2-e005

Automated Image Analysis Software: Valuable Tools for the Future?

Digvijay Singh, FAICO, MD, MBBS*

Division of Ophthalmology, Medanta-The Medicity, Gurgaon, Haryana 122001, India

Blindness causes significant disability and is associated with tremendous financial and social burden. Recent studies have shown an increase in the common causes of preventable blindness including irreversible diseases such as diabetic retinopathy and glaucoma. A study published in Lancet in 2012, highlighted the rise in Disability Affected Life Years (DALYs) between 1990 and 2010 by 160% for age related macular degeneration and 119% for glaucoma. In parallel, there has been a relative reduction in the ophthalmologist to population ratio as published in a recent article in the Canadian Journal of Ophthalmology in 2007. Developing countries face a worse situation, where the Ophthalmologist to population ratio is a dismal 1: several million depending. The situation is further compounded by the fact that in developing countries, nearly 70% of the population lives in rural areas while 70% of the ophthalmologists are based in urban areas. Providing accessible eye care is therefore a challenging task.

The goal of vision 2020 is to eliminate preventable blindness by the year 2020 and this mammoth endeavor is only possible with appropriate use of manpower and establishing eye care facilities in the peripheral and rural areas through vision centers or primary health care centers. Unlike the ophthalmologist to population ratio, which is rather dismal, the optometrist to population ratio in developing countries is slightly better being in the order of 1:600,000, though much worse than developed countries having a 1:10,000 ratio. This entails that, to achieve the goal of eliminating blindness, the optometrists and ophthalmic technicians would have to play a very significant role in disease screening and directing patients to the appropriate eye care facility.

It is at this step of screening that technology needs to be brought in to aid in disease detection and diagnosis. To take an example, we can examine a disease like glaucoma which has an estimated prevalence of 2.65% in people above 40 years of age and affects 60 million people worldwide, likely to increase to 80 million by 2020. Knowing that blindness due to glaucoma is irreversible and prevention is the sole option, and that the disease is asymptomatic and silent, the appropriate method of eliminating blindness due to it would be to perform preventive screening in the high risk age groups. For diagnosing the disease during population based screening, a relatively trained manpower is required, which is probably the biggest limiting factor to this kind of a screening exercise (particularly in developing countries). Thus, it is here that image analysis software [RIA-G (Kalpah innovations) or image recognition software (Watson, IBM Inc.) or many others in the research stage] would play a role, by highlighting suspect cases of glaucoma after processing fundus images. Many equipment have been devised to analyze retinal nerve fiber layer thickness for diagnosis of glaucoma but these are typically bulky and too expensive to put to use in a screening scenario. With the advent of highly portable fundus cameras at low costs, this problem is resolved and addition of automated disc analysis software to the cameras would enable a quick and effective screening process. Suspect patients could then be referred to an ophthalmic clinic where further testing to confirm the diagnosis and treatment can be done. The same process can also be conducted remotely over telemedicine but that would require an ophthalmologist to be viewing all the images for diagnosing. An automated software eliminates this need. Likewise, other automated image analysis software has been devised to detect diabetic retinopathy, retinopathy of prematurity, cataract, etc.

ISSN 2475-1278 http://dx.doi.org/10.17140/OOJ-2-e005

Automated image analysis software has been in the making for the last two decades. Initial attempts at developing these programs did not achieve much success due to varied reasons. Prominent among these were limitations of infrastructure such as poor resolution of fundus cameras, high costs of equipment, slow processing power of computers, absence of optical connectivity, etc. Most of these are not hurdles in development anymore. Other reasons for poor performance of these software included factors such as individual-to-individual variability of biological systems, association of glaucoma with other ocular diseases (myopia, diabetic changes and cataract) which act as confounding factors in analysis and the broad grey zone in establishing a clinical diagnosis of glaucoma. While these are difficult to overcome, some newer innovations are likely to help the next generation of image analysis software succeed more than their previous versions. The first of these is cloud computing. This concept entails installing the software on a cloud server and uploading fundus images onto that for analysis. The images and the results of the analysis are then available for the ophthalmologist to view from any location and also the patient can have an access to his data even if he wants multiple opinions or changes clinics. Sequential images can be compared for establishing a diagnosis or modulating therapy. For purposes of screening, a field technician can upload images onto the cloud, which can screen images and automatically seek opinion from an expert at a specialist centre for suspect cases to decide there and then whether a patient needs to be brought in for treatment. This is particularly important in large screening and outreach camps where a patient once missed may be very difficult to trace later. The other innovation is the ability of the software to learn from its own errors. This is sort of an artificial intelligence whereby when an ophthalmologist manually corrects a wrong analysis report, the software attempts to learn where it went wrong and avoid making the error a second time. This holds even more meaning when the software is on a cloud system and multiple users are analyzing thousands of images. As each user makes a correction, the software learns and corrects itself for all other users. Over a period of time, it would start to give near perfect results. This innovation is now finding way into the next gen software.

The future of imaging and image analysis looks exciting. The priority for developers is to provide low cost solutions, portable devices and multifunction equipment in line with the needs of the healthcare industry. While a lot has been done in the last decade and technology has advanced by leaps and bounds there is a lot, which is waiting to be done. A good example in this context is the incorporation of spectral imaging cameras in fundus imaging devices that can capture and show a great deal more than we can currently visualize. Standard stereoscopic imaging is likely to be a part of newer cameras and with the growing availability of three-dimensional viewing systems, this may not be too far in the future. Both these innovations of imaging would require software for analyzing what the human eye may not be able to see.

Ophthalmology is a highly technology dependent field. Next generation image analysis software are getting ready to help tackle blindness and change making ophthalmic diagnosis as we know it today. There is a lot happening out there in the world of medical technology, we have to embrace the new to move ahead.

THE OPHTHALMOLOGY OPEN JOURNAL

Openventio PUBLISHERS

ISSN 2475-1278 http://dx.doi.org/10.17140/OOJ-2-e006

Editorial

Corresponding author
Daniel H. Scorsetti, MD, PhD
Chairman and Professor
Department of Ophthalmology
Universidad del Salvador
Buenos Aires, Argentina
E-mail: dscorsetti@gmail.com

Volume 2 : Issue 1
Article Ref. #: 1000OOJ2e006

Article History
Received: January 4th, 2017
Accepted: January 20th, 2017
Published: January 20th, 2017

Citation
Scorsetti DH. Trifocal lenses for cataract surgery. *Ophthalmol Open J*. 2017; 2(1): e7-e8. doi: 10.17140/OOJ-2-e006

Trifocal Lenses for Cataract Surgery

Daniel H. Scorsetti, MD, PhD*

Department of Ophthalmology, Universidad del Salvador, Buenos Aires, Argentina

Since the introduction of the first intraocular lens in 1949, many technological advances have been made in order to optimize its design and construction. Owing to a number of recent advances and developement of modern lenses, it has now become possible to not only correct post-operative aphakia but also provide good visual acuity for far, intermediate and near distances by decreasing or eliminating eye glasses or contact lenses in majority of cases.

Apart from the above, modern intraocular lenses also reduce eye aberrations and protect the retina from ultraviolet (UV) radiation and the toxicity of blue light that are important factors to be taken care of in visual health.

Trifocal intraocular lenses surfaced for the 1st time in 2012 and continue to evolve and provide benefits to patients. Currently, we have 3 trifocal intraocular lenses which include:

- AT LISA tri 839MP (Carl Zeiss Meditec AG, Jena, Germany);
- PhysIOL (Finevision, Liège, Belgium);
- AcrySof® IQ PanOptix® (Alcon Research Ltd., Texas, USA).

These lenses have been approved by the European Union for use in adult patients with and without presbyopia who have cataracts and wish to reduce their dependency on eye glasses for far, intermediate and near distances.

We must know that both the PhysIOL and the AT LISA tri are hydrophilic lenses, whereas the AcrySof® IQ is hydrophobic. Although, the 3 trifocal lenses have the same functional characteristics to improve the visual acuity in the 3 distances, and thus reduce the use of optical aids, it is important to address the differences between them.

PanOptix® is a hydrophobic lens. Understanding the benefits and drawbacks of this characteristic the surgeon can accordingly choose the best suitable lens. Based on this, the 1st 2 lenses i.e. PhysIOL and the AT LISA tri can be implanted by 1.6 mm incisions while the hydrophobic needs a 2.2 mm incision but reduces the rate of post-operative capsular opacification. Hydrophilic lenses have shown less light scattering than the hydrophobic ones. While the PanOptix® lens has filters for blue light, no statistically significant differences were found in the published studies when compared to conventional lenses for light scattering.

An interesting concept is that of intermediate vision, which is a major point of difference in directing the choice of these lenses compared to the previous multifocal lenses. The PhysiOL and AT LISA tri have an intermediate focal point at 80 cm, while the PanOptix® lens has a focal point at 60 cm. Undoubtedly, the intermediate distance of 60 cm is much more user-friendly (than that of 80 cm) for computer users, allowing greater comfort in performing medium distance tasks among people who are in the working age or lead an active life.

With respect to the pre-surgical astigmatism that our potential patients may have experienced, we must know that the PhysiOL and AT LISA tri currently have toric options, which play a significant role in reducing the visual alterations that occur following the surgical intervention. However, since the patients were treated properly, they did not want to depend on post-operative air eyeglasses. Although, the PanOptix® lens has an excellent platform, known

ISSN 2475-1278 http://dx.doi.org/10.17140/OOJ-2-e006

by many as Acrysoft (fully tested with excellent results), it has no correction for astigmatism yet. Probably in the close future, Alcon will include the PanOptix® Toric models.

On the other hand, PanOptix® facilitates a greater transmission of light towards the retina since it allows 88% of the light to reach a pupil of 3 mm diameter in comparison with the PhysIOL lens that transmits 86% of the light to the same pupillary diameter. There is no data supporting this point with the AT LISA tri lens for that pupil size. This data is of great significance when assessing the contrast sensitivity and quality of vision observed by using these intraocular implants. Only one of the 3 trifocal lenses that comes preloaded is the AT LISA tri facilitating the loading maneuvers and avoiding contamination among the surgeons who prefer it.

Finally, although the 3 lenses are diffractive, one important difference is that the PanOptix® lens has a diffractive zone of 4.5 mm relative to the 5.0 mm zone of the other 2 trifocals. The 4.5 mm diffractive zone reduces the dependence of PanOptix® on the pupil size and/or brightness conditions to enable proper focusing on objects and to ensure normal vision.

There are some publications comparing results between bifocal lenses, extended range lenses (ABBOTT Symfony) and trifocal lenses.

The extended range lenses do not reach a near vision of quality relative to conventional bifocals or to modern trifocals as has been demonstrated in most studies, and is a common observation among the patients. Extended-range lenses work very well at intermediate and far distance but often fail to close when compared to other multifocal lenses.

There is a possibility that trifocal lenses will replace bifocals as they provide technological improvements, new designs, optimized platforms, and add an important intermediate focal point in operated patients who are in working and socially active conditions. A study published by Lee et al[1] showed that the patients who were operated with PanOptix® had better optical quality relative to those operated with the Restor +3 lens.

All lenses that have rings in their body generate similar discomforts in the form of halos, glare, etc., and the patients usually adapt to them. Thus, necessitating a good selection of the lenses.

AT LISA tri, in a study using a model eye of spherical aberration (with a 5 mm diameter pupil), indicated a large number of halos, although in clinical practice, there are no significant differences with respect to the adverse effects between the 3 trifocal lenses. Both halos and flashes tend to diminish over time, and generally after 6 months of surgery (or even much earlier), patients no longer complain about such discomforts, thus implicating the restoration of normal visión. The specialty offered by this clinical practice allows the recovery of the patient and the ability to see well at all distances, without any correction.

REFERENCE

1. Lee S, Choi M, Xu Z, Zhao Z, Alexander E, Liu Y. Optical bench performance of a novel trifocal intraocular lens compared with a multifocal intraocular lens. *Clin Ophthalmol*. 2016; 10: 1031-1038. doi: 10.2147/OPTH.S106646

THE OPHTHALMOLOGY OPEN JOURNAL

Openventio PUBLISHERS

ISSN 2475-1278 http://dx.doi.org/10.17140/OOJ-2-107

Research

*Corresponding author
Natalia I. Kurysheva, MD
Professor
Head of the Diagnostic Department
Ophthalmological Center of the Federal Medical and Biological Agency of Russia
Clinical Hospital No. 86
Gamalei St. 15, Moscow 123098
Russian Federation, Russia
E-mail: e-natalia@list.ru

Volume 2 : Issue 1
Article Ref. #: 1000OOJ2107

Article History
Received: July 15th, 2016
Accepted: August 19th, 2016
Published: August 22nd, 2016

Citation
Kurysheva NI. Does OCT angiography of macula play a role in glaucoma diagnostics? *Ophthalmol Open J*. 2016; 2(1): 1-11. doi: 10.17140/OOJ-2-107

Does OCT Angiography of Macula Play a Role in Glaucoma Diagnostics?

Natalia I. Kurysheva, MD*

Ophthalmological Center of the Federal Medical and Biological Agency of Russia, Clinical Hospital No. 86, Gamalei St. 15, Moscow 123098, Russia

ABSTRACT

Purpose: To assess vascularity of the macular area in patients with glaucoma using optical coherence tomography angiography (OCT-A) and evaluate the role of its examination in early glaucoma diagnosis.
Materials and Methods: Thirty-eight eyes of patients with the early stage of primary open-angle glaucoma (POAG), 27 eyes of patients with the advanced and far-advanced stages of POAG, and 22 eyes of age-matched healthy subjects were examined using spectral-domain OCT-A (SD-OCT-A) (RtVue xR Avanti with the AngioVue software, San Jose, CA, USA) in order to measure retinal thickness and angio flow density (AFD) retina in macula (an area bounded by a circle with a diameter of 3 mm), including fovea and parafovea regions (superficial and deep) of the inner retinal layers. The AFD disc and peripapillary flow density were measured in optic nerve head (ONH) and 750-µm-wide elliptical annulus extending from the optic disc boundary. Retrobulbar blood flow parameters, including ophthalmic artery (OA), central retinal artery (CRA), short posterior ciliary arteries (PCAs), central retinal vein (CRV), and vortex veins (VV), were measured by color doppler imaging (CDI). The average thickness of the ganglion cell complex (avg GCC), retinal nerve fiber layer (RNFL), and choroid, as well as the focal loss volume (FLV) and global loss volume (GLV) of GCC were measured by means of SD-OCT. Automated perimetry was performed using Humphrey perimeter (Carl Zeiss Meditec, Dublin, CA, USA). Corneal-compensated intraocular pressure (IOPcc) and corneal hysteresis (CH) were determined using ocular response analyzer. Mean ocular perfusion pressure (MOPP) was calculated by measuring IOP and arterial blood pressure (BP) immediately prior to OCT and using formula: MOPP = (2/3 diastolic BP + 1/3 systolic BP) × 2/3 – IOP.
Statistical analysis was performed using SPSS version 21 and MASS library in the R language. As a measure of the parameter's importance in distinguishing patient groups, a value of the adjusted standardized statistic of the Mann-Whitney test (z-value) and an area under the receiver operating characteristic (ROC) curve (AUC) were used.
Results: Although all structural parameters and indices of retrobulbar blood flow were reduced in early glaucoma as compared to the normal controls, the following parameters were the main discrepancy criteria when discriminating these patient groups: macular vascular density-AFD Retina Superficial Whole En Face (z=3.86, p<0.0001; AUC 0.8 (0.69-0.90) and macular thickness in the inferior sector ILM-RPE (z=3.86, p<0.0001; AUC 0.8 (0.69-0.91)). In discriminating early glaucoma from the advanced and far advanced stages of the disease, the most useful were: AFD Disc Peripapillary Inferior Temporalis (z=5.61, p<0.0001; AUC 0.94 (0.86-1.0)) and mean flow velocity in CRA (z=4.16, p<0.0001; AUC 0.81 (0.69-0.92)).
Conclusions: The present study revealed the significance of OCT-A for the early diagnosis of glaucoma and the priority of the investigation of the macular microcirculation and its thickness in the inferior sector. These results allow understanding the cause of the early involvement of the macular inner layers in the pathological process in glaucoma.

KEYWORDS: Primary open-angle glaucoma; Spectral-domain OCT-A (SD-OCT); Ocular blood flow; Optical coherence tomography angiography (OCT-A).

ISSN 2475-1278 http://dx.doi.org/10.17140/OOJ-2-107

ABBREVIATIONS: AFD: Angio Flow Density; AUC: Area Under ROC Curve; avg GCC: Average thickness of the ganglion cell complex; BP: arterial blood pressure; CDI: Color Doppler Imaging; CH: Corneal Hysteresis; CRA: Central Retinal Artery; CRV: Central Retinal Vein; CT: Choroidal Thickness; EDV: End Diastolic Velocity; FLV: Focal Loss Volume; GCC: Ganglion Cell Complex; GLV: Global Loss Volume; ILM: Inner Limiting Membrane; IOP: Intraocular pressure; IOPcc: corneal-compensated IOP; IPL: Inner Plexiform Layer; MD: Mean Deviation; MOPP: Mean Ocular Perfusion Pressure; MVZ: Macular Vulnerability Zone; OA: Ophthalmic Artery; OCT: Optical Coherence Tomography; OCT-A: Optical Coherence Tomography Angiography; ONH: Optic Nerve Head; PI: Pulsatility Index; POAG: Primary Open-Angle Glaucoma; PSD: Pattern Standard Deviation; PWD: Pulsed-Wave Doppler; RI: Resistive Index; RNFL: Retinal Nerve Fiber Layer; ROC curve: Receiver Operating Characteristic curve; RPE: Retinal Pigment Epithelium; SAP: Standard Automated Perimetry; SD-OCT: Spectral-Domain Optical Coherence Tomography; SD-OCT-A: Spectral-Domain Optical Coherence Tomography Angiography; SPCA: Short Posterior Ciliary Arteries; Vmean: mean velocity; VV: Vortex Vein.

RELEVANCE

In recent years increasing attention has been paid to the macular area in glaucoma diagnostics.[1,2] Although macula is less than 2% of the retina, it contains 30% of retinal ganglion cells (RGC).[3]

It has long been recognized that early glaucomatous damage can affect the macula.[4-9] Moreover there is a lot of evidence of even initial damage of the macula in glaucoma, which has been repeatedly cited for the past 40 years.[10-12] However, early macular damage has been ignored in clinical practice to a great extent until recently.

In 2010, Gabriele et al[13] obtained detailed data about the anatomy of glaucomatous damage of the macula by means of OCT. D. Hood introduced the concept of "the macular vulnerability zone (MVZ)"—a zone of the macula that is the most vulnerable in glaucoma.[14,15] Nevertheless, the origin of this phenomena is still unclear.

Reduced retinal hemoperfusion in glaucoma has been repeatedly mentioned in the literature.[16-18] However, the lack of a reliable method to measure the optic nerve head and macula microcirculation did not allow to clarify the role of circulatory disorders in glaucoma pathogenesis. A new 3D angiography algorithm (split-spectrum amplitude-decorrelation angiography, (SSADA)) was developed for imaging retinal microcirculation.[19] This method is based on ultrahigh-speed optical coherence tomography (OCT), and was called OCT-angiography (OCT-A). Using OCT-A the vascular density in the optic nerve head (ONH) and peripapillary area was measured.[19-21] The authors found reduced ONH blood vessel density that was associated with structural and functional glaucomatous damage.[22-25]

The purpose of the present study was to assess vascularity of the macular area in patients with glaucoma by means of OCT-A.

MATERIALS AND METHODS

Sixty-five eyes of patients with POAG were examined: 38 eyes with early glaucoma, 27 eyes with advanced and far-advanced glaucoma. The control group has been presented by 22 eyes of healthy age-matched subjects without any ophthalmic pathology (Table 1).

Glaucoma was diagnosed on the basis of characteristic changes in ONH that were detected by ophthalmoscopy: pathological deviation from the normal neural rim, glaucomatous optic disc cupping, peripapillary atrophy, wedge-shaped defects of RNFL adjacent to the edge of the optic disc, hemorrhages on the

Parameter	Normal controls	*p*-value*	POAG I	*p*-value**	POAG II-III	Total *p*-value***
N	22		38		27	
Age, years	61.9 (6.2)	0.622	62.5 (7.6)	0.367	64.8 (4.7)	0.071
Systolic BP, mmHg	126.6 (4.6)	0.010	135.4 (17.4)	0.472	130.9 (13.7)	0.018
Diastolic BP, mmHg	81.4 (6.9)	0.183	83.6 (9.9)	0.726	83.15 (8.2)	0.344
IOPcc, mmHg	15.5 (3.1)	0.001	19.4 (4.6)	0.549	19.4 (6.2)	<0.001
MOPP, mmHg	50.4 (2.4)	0.198	47.8 (9.8)	0.594	46.6 (7.7)	0.081
MD, dB	-0.03 (0.84)	<0.001	-1.95 (3.48)	<0.001	-12.13 (6.2)	<0.001
PSD, dB	1.41 (0.19)	0.006	2.20 (1.62)	<0.001	9.79 (3.59)	<0.001
RNFL, μm	101.9 (6.1)	<0.001	91.8 (10.3)	<0.001	69.3 (14.3)	<0.001
GCC, μm	98.3 (7.6)	0.001	89.2 (10.4)	<0.001	70.5 (10.4)	<0.001
FLV, %	0.21 (0.23)	0.004	2.18 (2.05)	<0.001	9.50 (3.68)	<0.001
GLV, %	1.62 (1.06)	0.001	7.60 (6.10)	<0.001	25.91 (9.44)	<0.001
Foveal CT, μm	312.3 (88.5)	0.342	279.9 (105.3)	0.906	276.6 (82.6)	0.581
Peripapillary CT, μm	181.4 (51.3)	0.348	179.3 (93.3)	0.472	161.9 (64.9)	0.346

The data are median; standard deviation is given in parentheses.
*actual level of significance (*p-value*) between the control group and POAG I
**_p-value_ between POAG I and POAG II-III
***_total p-value_, comparison of the three groups using Kruskal-Wallis rank test

Table 1: Patients characteristics.

ISSN 2475-1278 http://dx.doi.org/10.17140/OOJ-2-107

optic disc boundary. The results of standard automated perimetry (SAP) were outside normal limits.

Those patients who had previously used antiglaucoma drops were asked to discontinue the drug for a period of 3 weeks (drug washout period), while others were newly diagnosed glaucoma cases. Only one eye per patient was included in the study: in the glaucoma patients—the eye with a greater glaucomatous damage, and in the healthy individuals–the right eye.

All patients were Caucasians. The healthy participants were recruited from the persons accompanying the patients and had IOP of less than 21 mmHg for eyes, a normal Humphrey Swedish Interactive Threshold Algorithm (SITA) 24-2, standard visual field with mean deviation (MD) and pattern standard deviation (PSD) within 95% limits of the normal reference. They also had a Glaucoma Hemifield Test (GHT) within 97% limits, a central corneal thickness ≥500 μm, a normal-appearing ONH, a normal RNFL, an open anterior chamber angle as observed by gonioscopy, and no history of chronic ocular or systemic corticosteroid use. The age and race distribution of the controls matched that of the glaucoma patients.

The inclusion criteria were: ametropia ≤0.5 D and open anterior chamber angle of ≥30° confirmed by OCT of the anterior segment (Visante OCT, Zeiss). Only patients who had not undergone any eye surgery were included in the study. The exclusion criteria were: systemic administration of beta-blockers and calcium-channel blockers, concomitant ocular disease (except early-stage cataract), chronic autoimmune diseases, diabetes mellitus, acute circulatory disorders in past medical history, and any concomitant disease involving the administration of steroid drugs. A history of ocular arterial or venous obstruction (branch or central occlusion) or systemic conditions associated with venous congestion (e.g. heart failure) were also considered as exclusion criteria. All patients underwent Doppler ultrasound scanning to exclude pathology of the brachiocephalic vessels. Patients with normal tension glaucoma were excluded from the study.

IOP was measured using the ocular response analyzer (Reichert Ophthalmic Instruments, Depew, NY, USA). The device is based on a burst of air directed towards the cornea and uses two application pressure measurements, one during the depression of the cornea and another during the recovery. Measurement of CH allows for the calculation of IPOs, which appears to be less affected by properties of the cornea than conventional application goniometry.

OCT was performed using the RTVue-100 OCT (Optovue, Inc., Fremont, CA, USA) in the optic disc area (ONH protocols and 3D Disc) and macular area (GCC protocol) in tracking mode. RNFL was investigated in the ONH study protocol; three indices-avg GCC, FLV, and GLV were measured in the GCC protocol.

The choroidal thickness (CT) was investigated using the RTVue-100 OCT in tracking mode (Retina Cross Line protocol). CT was defined as a distance between the hyper reflective signal lines from the retinal pigment epithelium (RPE) to the continuous hyper eflective line on the sclera/choroid border. CT at the foveal center was obtained by averaging the results of measurement during vertical and horizontal scanning, a method that has been described in more detail previously.[26] For statistical processing of the CT at the foveal center, 13 measuring points in the area of 6×6 mm were selected. In addition, a point located 3 mm nasal from the foveal center in the direction of the disc center, i.e. at a point as close as possible to the peripapillary zone (pCT), was used for analysis.

The thickness of the macular area and RNFL in sectors and microcirculation parameters were measured in the peripapillary and macular areas using spectral-domain optical coherence tomography (SD-OCT) by means of RtVue XR Avanti (Optovue Inc., Fremont, CA, USA) with AngioVue function (OCT-A). Two vascular plexuses were studied during OCT-A: a *superficial plexus* located between the inner limiting membrane (ILM) (3 μm below its surface) and inner plexiform layer (IPL) (15 μm below its surface); and a *deep plexus* located in the retina from 15 μm to 70 μm below the ILM (Figure 1).

Two parameters were measured in the macular area: retinal thickness and relative vessel density of the retinal microvasculature-*AFD Retina*. AFD is the ratio of the area of the vessels in the test spot to the area of this spot (in %). Measurements were carried out in the foveal area (circumference with a diameter of 1 mm) and parafovea (in the area between the foveal border and a circumference 3 mm in diameter). The fovea and parafovea averaged value-*AFD Retina Whole En Face*–was measured as well.

Relative density of the ONH microvasculature (*AFD Disc Whole En Face*) was measured in ONH and peripapillary (750-μm-wide elliptical annulus extending from the optic disc boundary in the layer of 100 μm thickness from ILM), and only in the peripapillary area (*peripapillary vessel density*).

The method used for investigating blood flow velocity in retrobulbar vessels included gray-scale ultrasound, CDI and pulsed-wave doppler (PWD). The ultrasound examinations were performed with a VOLUSON 730 Pro-ultrasound system (GE Medical Systems Kretztechnik GmbH & Co OHG, Austria, Germany) and a SP 10-16 transducer. With the patient in supine position, sterile ophthalmic gel was applied as a coupling to the closed eyelid, and the probe was positioned gently with minimal pressure. The application of a gray-scale ultrasound enabled us to obtain the image of the globe and orbit. CDI was used to display the fine orbital vessels directly, including OA and its branches, CRA, the temporal and nasal PCAs, CRV, VV, and the superior ophthalmic vein (SOV). It was done according to the expected anatomical position of the vessels and its color code. The blood flow in the OA was evaluated at a depth of 35

THE OPHTHALMOLOGY OPEN JOURNAL

Openventio PUBLISHERS

ISSN 2475-1278 http://dx.doi.org/10.17140/OOJ-2-107

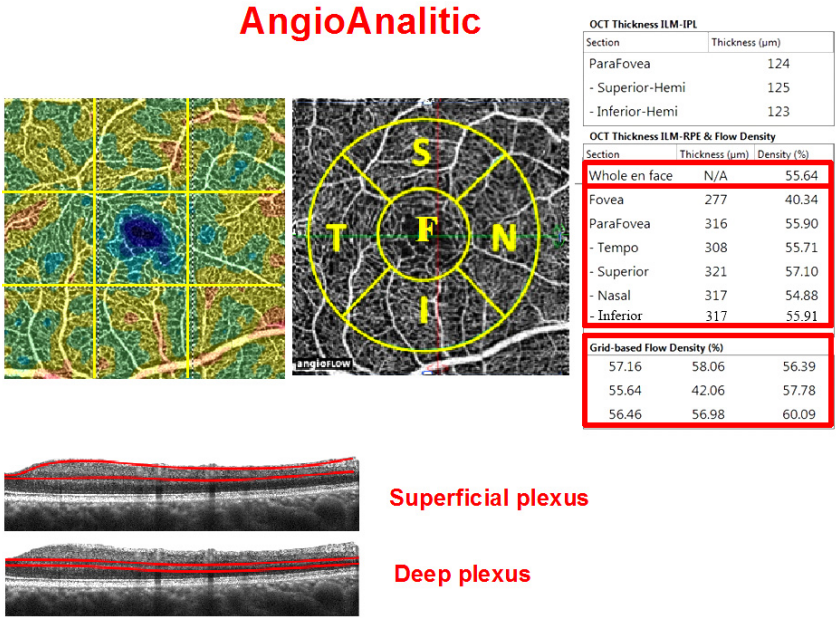

Figure 1: Macular vascular density protocol (AngioVue Retina protocol, RtVue XR Avanti device with AngioVue function) of a healthy eye. Top row: vascular density map (left), macula map by sectors (middle): F: fovea, S: parafovea superior, N: parafovea nasalis, I: parafovea inferior, T: parafovea temporalis. All five sectors together constitute the Whole En Face parameter. The table on the right: upper table-parafoveal thickness from ILM to IPL; table in the middle-macular thickness from ILM to RPE and relative vessel density (flow density) at the fovea and parafovea; bottom table-relative vessel density by sector (grid-based flow density) on the entire scan. Studied areas of the superficial and deep vascular plexuses on the B-scan are shown at the bottom.

mm. The CRA blood flow velocity was examined in the canal of optic nerve at the distance of 5-6 mm from the posterior wall of the globe. The PCAs were identified on either side of the optic nerve, about the same distance from the fundus as the CRA and CRV. By means of PWD we measured the blood flow spectrum of vessels and its main indices: peak systolic velocity (PSV), end-diastolic velocity (EDV), mean velocity (Vmean), resistive index (RI), and the pulsatility index (PI).

MOPP was calculated from IOP and BP measurements immediately before the OCT scanning and investigation of retrobulbar blood flow, after a 10-minute resting period in the sitting position. Systemic BP was measured using the Riva Rocci technique. MOPP was calculated using the formula:

MOPP = (2/3 diastolic BP + 1/3 systolic BP) × 2/3 – IOP.

Experimental Design

The study was approved by the ethical committee (Institutional Review Board, (IRB)) at the Institution of Federal Medical and Biological Agency of Russia and was conducted in accordance with Good Clinical Practice within the tenets of the Helsinki Declaration. Each patient/subject was required to sign an informed consent form before being enrolled in the study and prior to any measurements being taken.

In all subjects an ophthalmologic examination was performed including determination of visual acuity, biomicroscopy, applanation tonometry, gonioscopy, pachymetry, measurement of axial length and anterior chamber depth, and imaging of the anterior segment of the eye using OCT. Patients were instructed to avoid caffeine intake, smoking and exercise for 5 hours prior to the study visit.

Statistical Analysis

In the study, we used the two-tailed Wilcoxon rank sum test (Wilcoxon-Mann-Whitney test). Parameters with $p<0.05$ were considered statistically significant. As a measure of the parameter importance in distinguishing the groups, we used the absolute standardized z-value of the Mann-Whitney test and AUC by applying a logistic model with the parameter as a sole predictor. We excluded such parameters as IOPcc, MD, and PSD from the non-parametric analysis of variance (Non-parametric ANOVA) because the increased IOP and perimetric indices were considered when arranging groups of patients with POAG.

Since a number of parameters (GCC, GLV, systolic and mean perfusion pressure, CT) depended on the anterior-posterior axis and the age of the subjects, we adjusted these parameters on the basis of the linear regression model. In order to examine the relationship between the characteristics, we used the Spearman correlation coefficient. Statistical analysis was performed using the SPSS version 21 and MASS library in R.

RESULTS

Structural and functional parameters differed significantly between the treatment groups (Table 1).

All OCT-A parameters differed significantly between

ISSN 2475-1278 http://dx.doi.org/10.17140/OOJ-2-107

the patient groups. The variability of the OCT-A parameters in glaucoma was significantly more pronounced than in the normal controls (Figure 2). The most significant difference between the patients with primary glaucoma and healthy individuals was the capillary density in the superficial and deep vascular plexuses in the macula. The difference between the early stage and the advanced stages of glaucoma was less pronounced (Figures 2 and 3). It should be noted that the retinal thickness in the patients with early glaucoma differed significantly from the retinal thickness in the healthy subjects only in the lower sector (Table 2).

Tables 3 and 4 demonstrate the results of comparison of the groups. The most significant indicators in distinguishing early glaucoma from the normal controls were parameters of the macular region: macular thickness in the inferior parafoveal sector and capillary density in the superficial and deep vascular plexuses (Table 3). The reduction in the capillary density in the peripapillary retina, as well as the structural indicators (RNFL, GCC, GLV), was of less significance as compared to the above parameters. From Table 3 it can be concluded that the OCT-A blood flow parameters were of higher diagnostic value than the

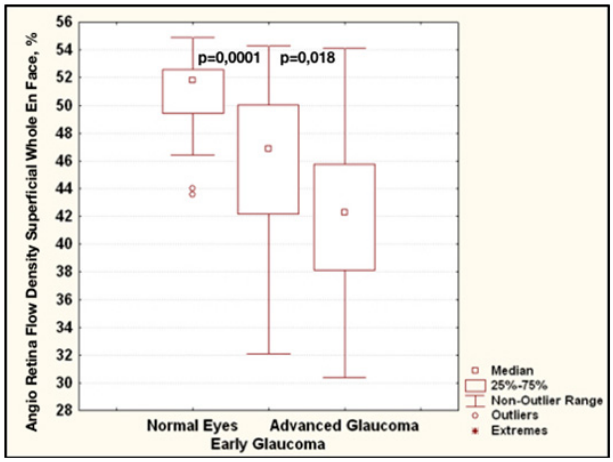

A. AFD Retina Superficial Whole En Face

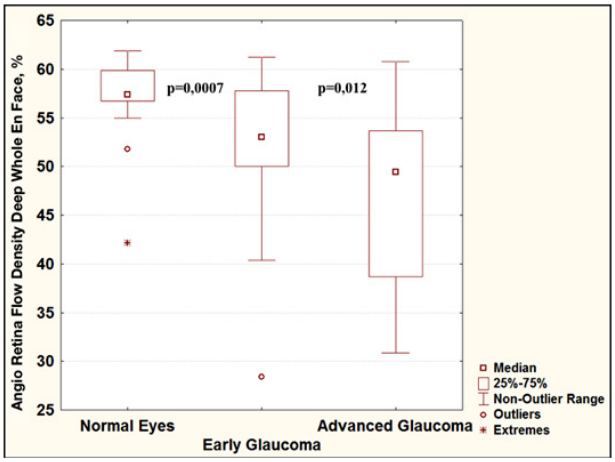

B. AFD Retina Deep Whole En Face

Figure 2: Diagrams comparing blood flow parameters in glaucoma according to OCT-A data: relative vessel density in the superficial (A) and deep (B) vascular plexuses of the macula. For each of the diagrams: on the left is normal controls, in the middle is early glaucoma, on the right are the advanced stages of glaucoma.

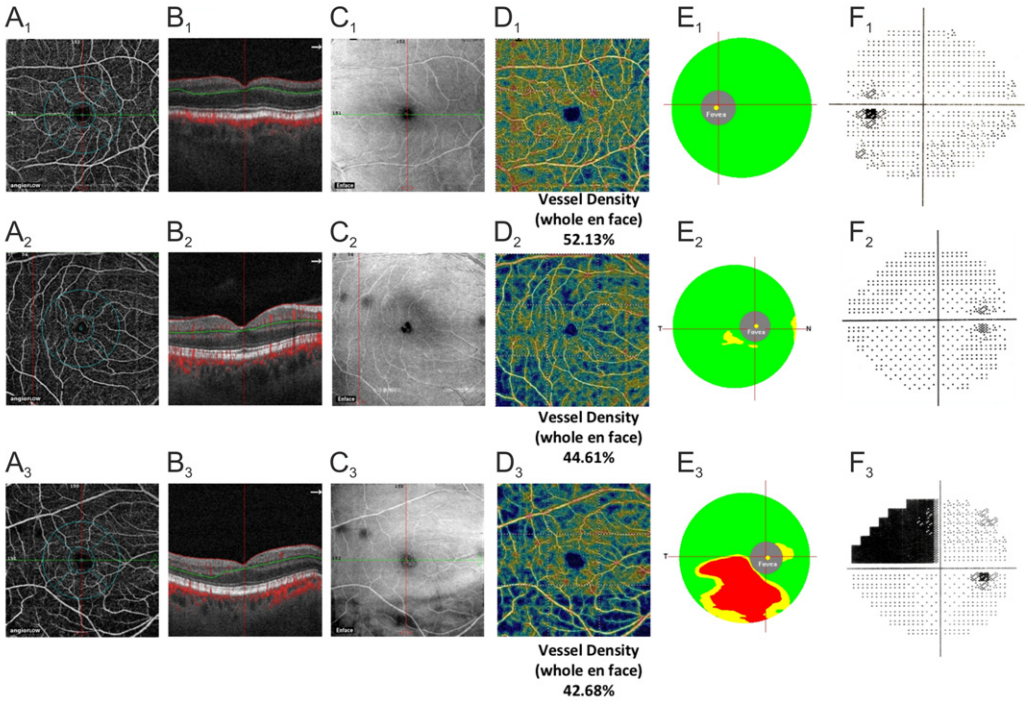

Figure 3: Clinical examples of the normal eye (A_1-F_1), early glaucoma (A_2-F_2), and advanced glaucoma (A_3-F_3). A_1-A_3: density map (AFD) of the microvasculature in the superficial plexus of the macula (3 **µm** below ILM to 15 µm below IPL). B_1-B_3: corresponding B-scans. C_1-C_3: corresponding En Face OCT images. D_1-D_3: color maps of the macular superficial plexus density. E_1-E_3: GCC color maps. F_1-F_3: SAP data.

ISSN 2475-1278 http://dx.doi.org/10.17140/OOJ-2-107

Parameter		Normal controls	*p*-value*	POAG I	*p*-value**	POAG II-III
ILM-RPE thickness, µm	Fovea	268.6 (13.3)	0.489	266.4 (18.5)	0.516	266.7 (35.0)
	Parafovea	322.3 (21.1)	0.112	309.5 (47.9)	<0.001	298.4 (22.5)
	-temporal sector	317.8 (22.9)	0.075	308.7 (23.5)	<0.001	287.1 (20.2)
	-superior sector	324.9 (21.6)	0.328	320.3 (23.2)	0.001	304.3 (26.0)
	-nasal sector	324.0 (20.8)	0.313	313.8 (47.9)	0.017	310.2 (29.2)
	-inferior sector	322.6 (21.2)	<0.001	240.8 (60.6)	0.737	291.8 (18.9)

The data are median; standard deviation is given in parentheses.
*actual level of significance (*p-value*) between normal controls and POAG I
***p-value* between POAG I and POAG II-III

Table 2: Retinal thickness from ILM to RPE in various macular sectors in the normal controls and in glaucoma.

Parameter	*z*-value	*p*-value	AUC	AUC LCL*	AUC UCL**
AFD Retina Superficial Whole En Face	**3.86**	**<0.0001**	**0.80**	**0.69**	**0.90**
Macula Thickness ILM-RPE parafovea inferior	**3.86**	**<0.0001**	**0.80**	**0.69**	**0.91**
AFD Retina Deep Whole En Face	3.31	0.0007	0.756	0.636	0.875
Peripapillary Vessel Density	3.189	0.001	0.747	0.626	0.868
avgGCC	3.09	0.002	0.74	0.60	0.88
RNFL	2.85	0.004	0.72	0.59	0.85
Temporal PCA, EDV	2.78	0,005	0.72	0.58	0.86
GLV	-2.66	0.007	0.7	0.57	0.87
CRV, EDV	2.4	0.02	0.7	0.54	0.86

The most important parameters that allow distinguishing early glaucoma from normal controls are given in bold.
*lower confidence limit of 95% confidence interval for AUC
**upper confidence limit of 95% confidence interval for AUC

Table 3: The most significant parameters in distinguishing early glaucoma from the normal controls.

Parameter	*z*-value	*p*-value	AUC	AUC LCL*	AUC UCL**
AFD Peripapillary Inferior Temporalis, %	5.61	<0.0001	0.94	0.86	1.0
CRA, Vmean, cm/sec	4.16	<0.0001	0.81	0.69	0.92

*lower confidence limit of 95% confidence interval for AUC
**upper confidence limit of 95% confidence interval for AUC

Table 4: The most significant indicators for differentiation between early and advanced stages of glaucoma.

parameters of retrobulbar blood flow. Because of the high correlation between the parameters from Table 3, for the differential diagnosis of early glaucoma from the normal controls we selected only those parameters that did not correlate (Table 3, given in bold). These two parameters demonstrated high sensitivity and specificity in early diagnosis of glaucoma, as can be seen from the ROC curves in Figure 4.

The most significant for the differential diagnosis of the stages of glaucoma were: the capillary density in the inferior peripapillary sector and mean blood flow velocity in CRA (Table 4).

We revealed a high correlation between the capillary density in the inner layers of the macular area and peripapillary retina and the GCC parameters (Table 5).

DISCUSSION

According to the results of the present study, the OCT-A parameters characterizing vascularity in the superficial and deep vascular plexuses of the macular area are of the highest value for the early diagnosis of glaucoma.

In the literature there are many indications that macular

ISSN 2475-1278 http://dx.doi.org/10.17140/OOJ-2-107

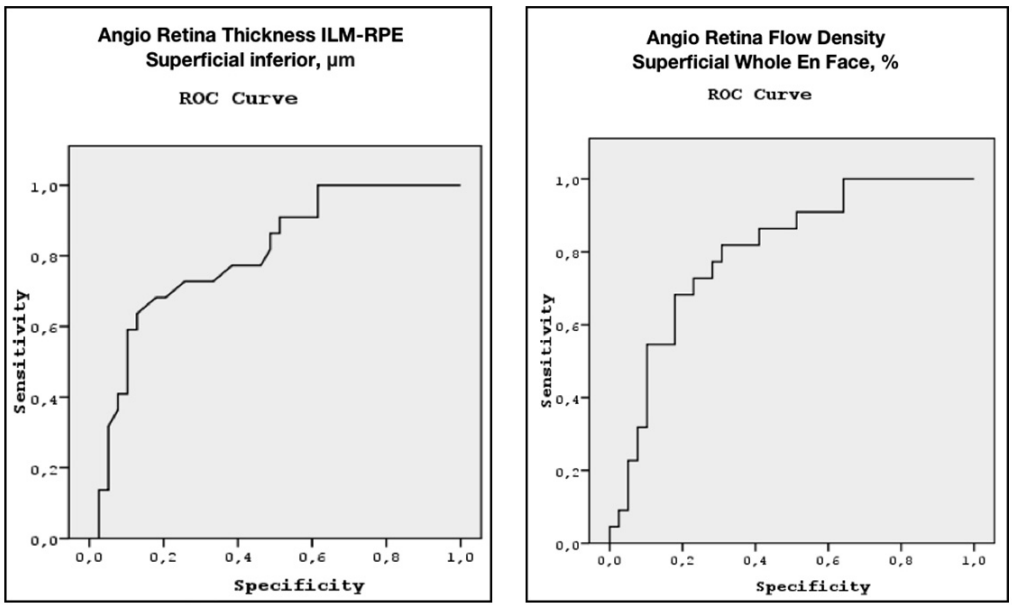

Figure 4: ROC curves for the Angio Retina Thickness ILM-RPE superficial inferior and Angio Retina Flow Density superficial Whole En Face.

Parameter	AFD Retina Superficial Parafovea	AFD Retina Superficial Whole En Face
GCC	r=0.481 p=0.003	r=0.486 p=0.002
GLV	r=-0.505 p=0.001	r=-0.505 p=0.001

Table 5: Correlation between the capillary density in the inner layers of the macular and the GCC parameters in early glaucoma.

area is involved in the process already at the very beginning of glaucoma. In 1984, Heijl and Lundqvist studied 45 eyes of patients with glaucoma progression and performed perimetry at 5˚, 10˚, 15˚, and 20˚ from the fixation point.[9] It was then when "the surprising prevalence of defects" at 5˚ from the center was noted for the first time, particular in the superior hemisphere of visual field. Authors drew a conclusion that early and even initial glaucomatous damage of visual field occurred in the macula and also in the area of arcuate defect typical of glaucoma. However, the causes of this phenomenon still remain unclear.

D. Hood introduced the concept of "the macular vulnerability zone (MVZ)"—a zone of the macula that is the most vulnerable in glaucoma.[14,15]

The origin of this however is still not clear. MVZ is described as a part of the relatively thick RNFL accurate region in healthy controls, as well as a part of the inferior disc region showing the most damage in glaucoma. That is, the axons from retinal ganglion cells in the inferior macular retina enter the high-risk inferior accurate region of the disc. This general region of the disc has the highest incidence of disc hemorrhages. They are often associated with glaucomatous damage. In fact, Park et al[27] observed that patients with damage within the central 10˚ on the 24-2 were more likely to have disc hemorrhages than those with comparable damage (nasal steps) outside the central 10˚.

Besides, this MVZ is just adjacent to a major inferior temporal artery or vein. This association may have no import other than the fact that the thickest part of the RNFL is associated with the major blood vessels. However, it is worth noting that there are hypodense regions (holes or tunnels) in the RNFL of glaucoma patients and suspects.[28] These hypodense regions are associated with visual field defects and may represent local axonal loss. Interestingly, they are almost always adjacent to a blood vessel.

It is still not entirely clear how these various findings are related, or which are most important in understanding the susceptibility of the inferior macular retinal ganglion cells to glaucomatous damage.

Thus, glaucomatous damage of the macula is common. It may appear at the early stage of the disease and may be not detected and/or underestimated when performing standard primary tests at the points located at a distance of 6˚ from each other. Besides the RNFL thinning in the accurate areas near ONH, the thinning of the inner macular layers can be seen already in suspected glaucoma, when the results of primary are classified as normal.

ISSN 2475-1278 http://dx.doi.org/10.17140/OOJ-2-107

To our knowledge, previously no attempt has been made to evaluate the macular vasculature in glaucomatous eyes by means of OCT-A.

Our results showed that the parameters of vessel density were significantly reduced in glaucoma not only in the superficial plexus supplying the GCC layer (Figure 3) but also in the deep vascular plexus as compared with healthy individuals of a similar age. Our previous studies demonstrated a reduction in the foveal choroidal thickness in glaucoma; this was indirectly indicative of the perfusion worsening in the macula.[26] However, OCT-A provided detailed information on blood supply to the inner layers of the retina in the macula and its outer layers due to the method's ability to perform a segmental evaluation of the blood flow. It can be assumed that trophic deterioration in these layers explains the involvement of the macula in the pathological process at the very beginning of the disease.

The most valuable criteria for the diagnosis of glaucoma have been searched forover the years. The importance of a combination of the structural and functional changes in the early diagnosis and monitoring of glaucoma has been repeatedly emphasized in the literature.[29-32]

For the same purpose we performed a comparative analysis of the structural and circulatory parameters in our recent studies and revealed a high diagnostic value of the retrobulbar blood flow parameters in the early diagnosis of glaucoma.[33] In the present study, along with the analyzed parameters, we for the first time studied the parameters of the ONH microcirculation, peripapillary retina and macula obtained by OCT-A. The OCT-A method is based on measuring *the degree of the amplitude decorrelation (difference)* at a certain point of the optical B-scan when obtaining multiple consecutive B-scans (split-spectrum amplitude-decorrelation angiography-SSADA). OCT-A is aimed at the selection of blood vessels from the surrounding tissue through the entire scanning depth without any contrast agents.[34]

The retina has three levels of blood supply (plexuses): radial peripapillary capillary plexus, superficial and deep plexuses.[35] All three of these vascular plexuses provide blood supply to the inner half of the retina, while the outer half of the retina receives blood supply from choriocapillaries. The main role in the supply to the RNFL is played by capillaries of the radial superficial peripapillary plexus, and to the retinal ganglion cells-by blood vessels of the superficial plexus. By means of OCT-A, Savastano et al[24] described localization of the superficial plexus at the GCC level and deep plexus in the outer plexiform layer. In the present study, we applied OCT-A to study the hemoperfusion of all the three plexuses in glaucoma.

In the literature, data on the use of OCT-A in glaucoma are scarce and limited to the results of the ONH and peripapillary retina study.[19-25] For example, Jia et al[19] studied the percentage area occupied by vessels (vessel density) in the optic disc and revealed that preperimetric glaucoma (PPG) patients had significant reductions of ONH perfusion compared to normal: the vessel density was reduced by 34% in the PPG group (p<0.05) with the repeatability 6.2%. The authors concluded that OCT angiography could detect the abnormalities of ONH perfusion and reveal the ONH blood flow mechanism related to glaucoma. Liu et al[20] also revealed a significant decrease in the peripapillary vessel density in patients with glaucoma as compared with healthy subjects of similar age. In the authors' opinion, this parameter was of high diagnostic value for early detection of glaucoma. The possible role of OCT-A in glaucoma monitoring was demonstrated in the recent studies by Wang et al[21,22] and Lévêque et al.[23] The authors found a significant decrease in the ONH vessel density in advanced glaucoma patients as compared with healthy subjects, as well as its correlation with MD, RNFL, and GCC thickness, but only in POAG and not in the normal controls. According to Lévêque et al,[23] the temporal sector of ONH is a critical study region for monitoring progression of glaucoma patients. The authors concluded that reductions in ONH blood flow detectable by OCT angiography might precede detectable visual field damage, hence, the vessel density of ONH had the power to differentiate normal eyes from eyes with POAG. It is important to note that in the mentioned studies glaucoma subjects had not stopped taking hypotensive eye drops before the examination although it is known that they may influence on ocular blood flow.

The present study demonstrates that the OCT-A has a diagnostic value in determination of the macular vascular density for the early glaucoma detection. This parameter exceeds the diagnostic value of peripapillary vessel density and RNFL thickness in the logistic model (Table 3). On the other hand, the vessel density in the peripapillary inferior temporal region had the highest diagnostic value for differentiation between the early and advanced stages of glaucoma (Table 4). One could speculate that the reduction of vascular density in the inner macula may precede the loss of ganglion cells and their axons. Moreover, it can be an example of the inter individual variation of vascularity that has been described by Hayreh S.[36] During his research in 100 human specimens, he did not find two identical patterns even in two eyes of the same person. Blood supply to the macula is derived from the choroid, which capillary network takes its origin from the PCA. It is evident that it is only the PCA circulation in the ONH that is relevant to the various ischemic disorders of the ONH and may be of high relevance in glaucoma. When the tissue is supplied by two or more end-arteries, the border between the distribution areas of any two end-arteries is called a "watershed zone". The significance of the watershed zones is that in the event of a fall in the perfusion pressure in the vascular bed of one or more of the end-arteries, the watershed zone, being an area of comparatively poor vascularity, is the most vulnerable to ischemia. Fluorescein fundus angiographic studies performed by Hayreh S. both in healthy and glaucoma patients have clearly shown that the PCAs and their subdivisions were end-arteries, right down to the choroidal arterioles. Thus, there are watershed zones between the distributions of the various PCAs. Hayreh S[37]

ISSN 2475-1278 http://dx.doi.org/10.17140/OOJ-2-107

emphasized that location of the watershed zone in relation to the ONH was the key to any discussion of ischemic disorders of the ONH. There is marked inter individual variation in the number and pattern of supply by the PCAs-the main source of blood supply to the ONH. Therefore, the pattern of distribution by the PCAs in the choroid and ONH is extremely variable.[38]

In this regard, OCT-A might become an important method for the individual evaluation of the capillary density in retinal tissue. According to the results of our study, the investigation of the vessel density in the superficial and deep vascular plexuses of the macular area might be of high priority for the glaucoma diagnosis and monitoring. The obtained highly significant correlation of the macular vascularity with the GCC structural characteristics (Table 5) agrees with the established fact: GLV has been as well recognized as one of the important diagnostic parameters in differentiating early glaucoma from the normal controls.[39]

Several limitations must to be considered when discussing the results of the present study. The first limitation is a relatively low number of patients. We used a non-parametric Wilcoxon-Mann-Whitney test to discover the difference between the groups because some variables have skewed distributions. Therefore, our results need to be confirmed in larger patient populations.

The limitations of the OCT angiography also should be considered when interpreting the results. They are: the influence of motion artifacts, shadowing effects, the difficulties of the localization of changes and the quantification of blood flow. The wavelength dependence is still present in OCT angiography. Besides OCT angiography cannot distinguish between perfusion reduction caused by tissue loss (a result of glaucoma) and ischemia (a cause of glaucoma). However, the OCT structural images can measure tissue loss. Thus, structural imagery and perfusion measurements could provide complementary information for both clinical assessment and pathophysiological investigation.

Careful attention should be paid to the interpretation of the CDI data as the subjective aspects of the CDI measurements have been pointed out in literature.[40] Harris et al[41] initially found that reproducibility was good in the CRA and OA, but had a higher variability in short PCA; the reproducibility of the CDI parameters in VV was not evaluated. Generally, data obtained in CRV is considered to be less reproducible. While CDI is highly examiner-dependent, the examiner was not blinded to the patients/subjects in present study. The fact that the examiner was not masked to the diagnosis is the limitation of the present study.

The next limitation is the IOP data. After drug washout period, IOP was significantly higher in glaucomatous eyes compared to normal controls, as demonstrated in the Table 1. This could affect the ocular blood flow parameters. However, we have not revealed any correlation between IOP and the parameters of microcirculation measured by OCT-A or CDI in glaucoma and the normal subjects.

CONCLUSIONS

The present study revealed the significance of OCT-A for the early diagnosis of glaucoma and the priority of the investigation of the macular microcirculation and its thickness in the inferior sector. These results allow understanding the cause of the early involvement of the macular inner layers in the pathological process in glaucoma.

ACKNOWLEDGMENT

The author thanks Dr. Ekaterina Maslova and Dr. Anna Trubilina for their generous and valuable assistance in examining of the patients and collecting scientific data.

REFERENCES

1. Leung CK, Ye C, Weinreb RN, et al. Impact of age-related change of retinal nerve fiber layer and macular thicknesses on evaluation of glaucoma progression. *Ophthalmology*. 2013; 120(12): 2493-2500. doi: 10.1016/j.ophtha.2013.07.021

2. Arintawati P, Sone T, Akita T, Tanaka J, Kiuchi Y. The applicability of ganglion cell complex parameters determined from SD-OCT images to detect glaucomatous eyes. *J Glaucoma*. 2013; 22(9): 713-718. doi: 10.1097/IJG.0b013e318259b2e1

3. Curcio CA, Allen KA. Topography of ganglion cells in human retina. *J Comp Neurol*. 1990; 300(1): 5-25. doi: 10.1002/cne.903000103

4. Aulhorn E, Harms M. Early visual field defects in glaucoma. In: Leydhecker W, ed. *Glaucoma, Tutzing Symposium.* Basel, Switzerland: Karger; 1967: 151-186.

5. Aulhorn E, Karmeyer H. Frequency distribution in early glaucomatous visual field defects. *Doc Ophthalmol Proc Ser*. 1977; 14: 75-83.

6. Drance SM. Some studies of the relationships of hemodynamics and ocular pressure in open-angle glaucoma. *Trans Ophthalmol Soc UK*. 1969; 88: 633-640.

7. Nicholas SP, Werner EB. Location of early glaucomatous visual field defects. *Can J Ophthalmol*. 1980; 15: 131-133.

8. Anctil J-L, Anderson DR. Early foveal involvement and generalized depression of the visual field in glaucoma. *Arch Ophthalmol*. 1984; 102(3): 363-370. doi: 10.1001/archopht.1984.01040030281019

9. Heijl A, Lundqvist L. The frequency distribution of earliest glaucomatous visual field defects documented by automated pe-

ISSN 2475-1278 http://dx.doi.org/10.17140/OOJ-2-107

rimetry. *Acta Ophthalmol*. 1984; 62(4): 657-664. doi: 10.1111/j.1755-3768.1984.tb03979.x

10. Anctil JL, Anderson DR. Early foveal involvement and generalized depression of the visual field in glaucoma. *Arch Ophthalmol*. 1984; 102(3): 363-370. doi: 10.1001/archopht.1984.01040030281019

11. Jeong J, Kang M, Kim S. Pattern of macular ganglion cell-inner plexiform layer defect generated by spectral-domain OCT in glaucoma patients and normal subjects. *J Glaucoma*. 2015; 24: 583-590. doi: 10.1097/IJG.0000000000000231

12. Drance S. The early field defects in glaucoma. *Invest Ophthalmol*. 1969; 8: 84-91. Web site. http://iovs.arvojournals.org/article.aspx?articleid=2203508. Accessed July 14, 2016

13. Gabriele ML, Wollstein G, Ishikawa H, et al. Three dimensional optical coherence tomography imaging: advantages and advances. *Prog Retin Eye Res*. 2010; 29(6): 556-579. doi: 10.1016/j.preteyeres.2010.05.005

14. Hood DC, Raza AS, de Moraes CG. Glaucomatous damage of the macula. *Prog Retin Eye Res*. 2013; 32: 1-21. doi: 10.1016/j.preteyeres.2012.08.003

15. Hood DC, Raza AS, de Moraes CGV, et al. Initial arcuate defects within the central 10 degrees in glaucoma. *Invest Ophthalmol Vis Sci*. 2011; 52(2): 940-946. doi: 10.1167/iovs.10-5803

16. Anderson DR. What happens to the optic disc and retina in glaucoma. *Ophthalmology*. 1983; 90(7): 766-770. doi: 10.1016/S0161-6420(83)34490-0

17. Schmidl D, Werkmeister R, Garhöfer G, Schmetterer L. Ocular perfusion pressure and its relevance for glaucoma. *Klin Monbl Augenheilkd*. 2015; 232(2): 141-146. doi: 10.1055/s-0034-1383398

18. Konieczka K, Ritch R, Traverso C, et al. Flammer syndrome. *EPMA J*. 2014; 5: 11. doi: 10.1186/1878-5085-5-11

19. Jia Y, Morrison JC, Tokayer J, et al. Quantitative OCT angiography of optic nerve head blood flow. *Biomed Opt Express*. 2012; 3(12): 3127-3137. doi: 10.1364/BOE.3.003127

20. Liu L, Jia Y, Takusagawa H, Morrison J, Huang D. Optical coherence tomography angiographyof theperipapillary retina in glaucoma. *JAMA Ophthalmol*. 2015; 133(9): 1045-1052. doi: 10.1001/jamaophthalmol.2015.2225

21. Wang Y, Fawzi AA, Varma R, et al. Pilot study of optical coherence tomography measurement of retinal blood flow in retinal and optic nerve diseases. *Invest Ophthalmol Vis Sci*. 2015; 52(2): 840-845. doi: 10.1167/iovs.10-5985

22. Wang X, Jiang C, Ko T, et al. Correlation between optic disc perfusion and glaucomatous severity in patients with open-angle glaucoma: An optical coherence tomography angiography study. *Graefes Arch Clin Exp Ophthalmol*. 2015; 253(9): 1557-1564. doi: 10.1007/s00417-015-3095-y

23. Lévêque PM, Zéboulon P, Brasnu E, Baudouin C, Labbé A. Optic disc vascularization in glaucoma: Value of spectral-domain optical coherence tomography angiography. *J Ophthalmol*. 2016; 2016: 6956717. doi: 10.1155/2016/6956717

24. Savastano M, Lumbroso B, Rispoli M. In vivo characterization of retinal vascularization morphology using optical coherence tomography angiography. *Retina*. 2015; 35(11): 2196-2203. doi: 10.1097/IAE.0000000000000635

25. Chen CL, Bojikian KD, Gupta D, et al. Optic nerve head perfusion in normal eyes and eyes with glaucoma using optical coherence tomography-based microangiography. *Quant Imaging Med Surg*. 2016; 6(2): 125-133. doi: 10.21037/qims.2016.03.05

26. Kurysheva NI, Ardzhevnishvili TD, Kiseleva TN, Fomin AV. The choroid in glaucoma: The results of a study by optical coherence tomography [In Russian]. *National Journal Glaukoma.* 2013; 4: 73-83.

27. Park SC, De Moraes CG, Teng CC, Tello C, Liebmann JM, Ritch R. Initial parafoveal versus peripheral scotomas in glaucoma: risk factors and visual field characteristics. *Ophthalmology*. 2011; 118(9): 1782-1789. doi: 10.1016/j.ophtha.2011.02.013

28. Xin D, Talamini CL, Raza AS, et al. Hypodense regions ("holes") in the retinal nerve fiber layer in frequency-domain OCT scans of glaucoma patients and suspects. *Invest Ophthalmol Vis Sci*. 2011; 52(10): 7180-7186. doi: 10.1167/iovs.11-7716

29. Harwerth RS, Wheat JL, Fredette MJ, Anderson DR. Linking structure and function in glaucoma. *Prog Retin Eye Res*. 2010; 29(4): 249-271. doi: 10.1016/j.preteyeres.2010.02.001

30. Medeiros FA, Lisboa R, Weinreb RN, Girkin CA, Liebmann JM, Zangwill LM. A combined index of structure and function for staging glaucomatous damage. *Arch Ophthalmol*. 2012; 130(9): 1107-1116. doi: 10.1001/archophthalmol.2012.827

31. Sung KR, Sun JH, Na JH, et al. Progression detection capability of macular thickness in advanced glaucomatous eyes. *Ophthalmology*. 2012; 119(2): 308-313. doi: 10.1016/j.ophtha.2011.08.022

32. Gardiner SK, Johnson CA, Demirel S. The effect of test variability on the structure-function relationship in early glaucoma. *Graefes Arch Clin Exp Ophthalmol*. 2012; 250(12): 1851-1861. doi: 10.1007/s00417-012-2005-9

33. Kurysheva NI, Irtegova EY, Parshunina OA, Kiseleva TN,

ISSN 2475-1278 http://dx.doi.org/10.17140/OOJ-2-107

Ardzhevnishvili TD. The search for new markers in the early diagnosis of primary open-angle glaucoma [In Russian]. *Russian Ophthalmological Journal*. 2015; 3: 23-29.

34. Spaide R, Klancic J, Cooney M. Retinal vascular layers imaged by fluorescein angiography. *JAMA Ophthalmol*. 2015; 133(1): 45-50. doi: 10.1001/jamaophthalmol.2014.3616

35. Snodderly D, Weinhaus R, Choi J. Neural-vascular relationships in central retina of macaque monkeys (Macaca fascicularis). *J Neurosci*. 1992; 12(4): 1169-1193. Web site. http://www.jneurosci.org/content/12/4/1169.long. Accessed July 14, 2016

36. Hayreh SS. Inter-individual variation in blood supply of the optic nerve head. Its importance in various ischemic disorders of the optic nerve head, and glaucoma, low-tension glaucoma and allied disorders. *Doc Ophthalmol*. 1985; 59(3): 217-246. doi: 10.1007/BF00159262

37. Hayreh SS, Podhajsky P, Zimmerman MB. Role of nocturnal arterial hypotension in optic nerve head ischemic disorders. *Ophthalmologica*. 1999; 213: 76-96. doi: 10.1159/000027399

38. Hayreh SS. Physiological anatomy of the choroidal vascular bed. *Int Ophthalmol*. 1983; 6(2): 85-93. doi: 10.1007/BF00127636

39. Arintawati P, Sone T, Akita J, Tanaka J, Kiuchi Y. The applicability of ganglion cell complex parameters determined from SD-OCT images to detect glaucomatous eyes. *J Glaucoma*. 2013; 22(9): 713-718. doi: 10.1097/IJG.0b013e318259b2e1

40. Ciulla T, Regillo C, Harris A. Retina and optic nerve imaging. In: Ciulla T, ed. *Retina and Optic Nerve Imaging*. Philadelphia, USA: Lippincott Williams & Wilkins; 2003: 245-254.

41. Harris A, Williamson T, Martin B, et al. Test/Retest reproducibility of color Doppler imaging assessment of blood flow velocity in orbital vessels. *J Glaucoma*. 1995; 4(4): 281-286. Web site. http://journals.lww.com/glaucomajournal/Abstract/1995/08000/Test_Retest_Reproducibility_of_Color_Doppler.11.aspx. Accessed July 14, 2016

THE OPHTHALMOLOGY OPEN JOURNAL

Openventio PUBLISHERS

ISSN 2475-1278 http://dx.doi.org/10.17140/OOJ-2-108

Mini Review

Corresponding author
Joy Sarkar, PhD
Department of Ophthalmology and Visual Sciences
University of Illinois at Chicago
Illinois Eye & Ear Infirmary
Chicago, IL 60612, USA
E-mail: jsarkar1@uic.edu

Volume 2 : Issue 1
Article Ref. #: 1000OOJ2108

Article History
Received: December 20th, 2016
Accepted: February 6th, 2017
Published: February 7th, 2017

Citation
Sarkar J. Recent perspectives on corneal nerves: A short review. *Ophthalmol Open J*. 2017; 2(1): 12-19. doi: 10.17140/OOJ-2-108

Recent Perspectives on Corneal Nerves: A Short Review

Joy Sarkar, PhD*

Department of Ophthalmology and Visual Sciences, University of Illinois at Chicago, Illinois Eye & Ear Infirmary, Chicago, IL 60612, USA

ABSTRACT

This mini-review provides an overview of recent trends in our understanding of the general structure of the cornea, the importance of corneal nerves, their function and distribution in the different layers of the cornea based on reports obtained by imaging techniques such as *in vivo* confocal microscopy (IVCM) and immunohistochemistry (IHC) analysis. Recent data on corneal nerve status in conditions such as Dry Eye Disease (DED) and Diabetes is also discussed. There is additional emphasis on corneal nerve damage due to injury especially during surgical interventions and underlying disease states as well as translational research on corneal nerve regeneration. Information on recent clinical studies on the effect of laser corneal surgery and its impact on corneal nerves is also presented.

KEY WORDS: Corneal nerves; Immunohistochemistry (IHC); Dry Eye Disease (DED).

ABBREVIATIONS: IVCM: *In Vivo* Confocal Microscopy; IHC: Immunohistochemistry; Dry Eye Disease (DED); TEM: Transmission Electron Microscopy; LASIK: Laser-assisted *in situ* keratomileusis; PRK: Photorefractive keratectomy: ReLEx: Refractive Lenticule Extraction; SMILE: Small Incision Lenticule Extraction.

INTRODUCTION

The eye is one of the most fascinating organs of the human body and has numerous parts each of which plays a critical role in providing vision (sight). As the well-known saying goes "the eyes are the window to the soul", for the layman, the cornea is indeed that part of this window through which light enters the eye and along with the lens is focused onto the retina. The retina in turn absorbs and converts the light into electrochemical impulses which are then transferred to the brain *via* the optic nerve. The cornea is the outermost transparent, clear and avascular connective tissue layer that forms the front part of the eye. It is dome-shaped and covers the pupil, iris and the anterior chamber and acts as a structural barrier for primary infections to the eye. Structurally and anatomically the main layers of the human cornea include, the epithelial layer or epithelium, the Bowman's membrane, the stromal layer or stroma, the recently identified Pre-Descemet's layer known as Dua's layer, the Descemet's membrane and the endothelial layer or endothelium.[1-3] The cornea stands out as being one of the most densely innervated tissues in the body[4] and our current understanding of the cornea and corneal diseases in general is based on the seminal works of numerous scientists and clinicians in the field of ophthalmology. The purpose of this short review is to highlight some important studies and findings in the field of corneal nerve research.

STRUCTURE AND FUNCTION OF CORNEAL NERVES

The organization of human corneal nerves has been investigated ever since Schlemm et al[5] discovered their presence in the limbus. Corneal nerves originate from the trigeminal nerve (ophthalmic branch) and enter the corneal stroma after which they form a subbasal plexus below the epithelium, and extend into thinner nerves containing nociceptors at the corneal surface.[6,7] The

ISSN 2475-1278 http://dx.doi.org/10.17140/OOJ-2-108

Figure 1: Schematic Representation of Corneal Nerves.
Panel A: Branched subbasal and stromal nerves are distributed throughout the cornea with the subbasal nerves visible on the corneal surface whereas the stromal nerve trunks are deeper. Panel B: Cross-sectional view of corneal stromal nerves and subbasal plexus in the cornea. The beaded nerves fibers separate from the subbasal plexus and obliquely/slantwise protrude upwards towards the epithelium and form terminal nerve fibers in the superficial layers of the corneal epithelium (schematic artwork done by Joy Sarkar and Ruth Zelkha based on Linda JM et al, 2003 and Tomas-Juan J et al, 2014).[4,46]

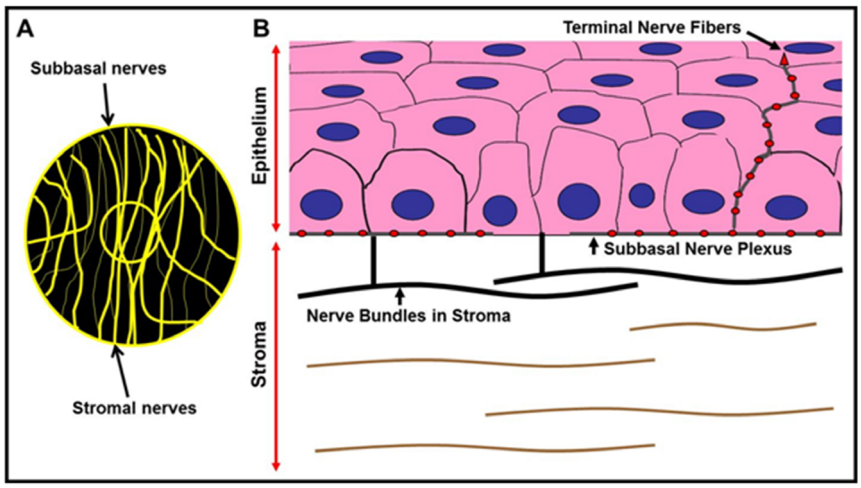

innervations of the cornea and bulbar conjunctiva is contributed mainly by the sensory fibers of the ophthalmic branch of the trigeminal nerve and by the less numerous sympathetic and parasympathetic nerve fibers.[8] In addition to their important sensory function, corneal nerves also play an important role in providing protection and are involved in trophic functions. Corneal nerves have also been known to be involved in the regulation of corneal epithelial integrity, wound healing and cell proliferation.[9] A renewed interest in corneal neurobiology arose recently because of the pivotal role these nerves play in maintaining a healthy ocular surface, which is especially important today due to the damage corneal nerves incur from refractive surgery, corneal transplants and herpetic infections (Figure 1).

Corneal Nerves and Dry Eye Disease

One major condition that causes epithelial abnormalities is dry eye syndrome. It is has been estimated that nearly 10% of the U.S. population suffers from dry eye syndrome, which in turn significantly affects quality of life in these patients. Dry Eye Disease (DED) is considered to be a disease mainly of the tears and ocular surface causing symptoms of discomfort, disturbance in vision and instability of the tear film with possible damage to the ocular surface.[1] DED can also occur due to disturbance of the lacrimal glands, the ocular surface and eyelids, and the sensory and motor nerves that connect them.[8,9] A stimulation of corneal nerves followed by nerve alterations has been postulated as one of the core pathophysiological mechanisms in DED.

Corneal Nerves and Aging

Aging has been implicated in the increased incidence of dry eye[10] and although some risk factors have been identified, not much is known about the causes. The role of aging and how it affects nerve architecture of the cornea is a very important focus of recent research. Early studies on corneal nerves in animals and humans were purely based on light or electron microscopic evaluations. Schimmelpfennig et al[11] studied fresh central corneal buttons from keratoplasties and enucleations by staining with gold chloride and provided one of the first comprehensive descriptions of corneal epithelial nerves.[11] This has been followed by numerous fixation and staining methodologies and this gamut of analytical procedures have greatly contributed to enhancing our knowledge of the morphology, ultrastructural organization, density, and corneal nerve alterations after injury or death.[4,6] Studies by two prominent groups[12,13] mention that 'aging' is accompanied by structural and functional changes in the cornea involving corneal steepening and increased thickness of the Descemet's membrane.[14] Aging has also been shown to impact corneal wound healing as well as affect visual acuity and refractive outcomes after laser refractive surgery.[15-18]

Imaging and Visualizing Corneal Nerves

For the longest time, visualization of the human cornea and the different layers within has remained a pipe-dream. In recent years, the introduction of *in vivo* confocal microscopy (IVCM) has provided a new method for high resolution corneal examination in living patients.[19,20] It has broadened the scope for non-surgical intervention and cellular examination of live corneas *in vivo*.[21-26] However, despite breakthroughs in imaging techniques, the distribution of corneal nerves is not completely deciphered as yet and the reasons for this lack of understanding is because of the difficulty in obtaining detailed innervations in the different corneal layers since conventional histology requires fresh corneas. Secondly, transmission electron microscopy (TEM) images are

ISSN 2475-1278 http://dx.doi.org/10.17140/OOJ-2-108

restricted to very tiny areas of the corneal surface (0.1 mm^2). Finally, IVCM images of the human cornea are captured from the corneal apex. Also these microscopes have a limitation in that they cannot image branching nerves and their terminals of diameters <0.5 mm.

In a recent paper published by Haydee Bazan's group at LSU, New Orleans, LA, USA,[27] the authors have introduced a novel tissue preparation technique to study and image the exact location of nerve fibers. Studies in the past used cross-sections which failed to show detailed corneal innervations. Studies by Müller et al have implicated nerve degeneration to be the main reason for lack of innervation data as seen *via* electron microscopy techniques demonstrating significant nerve degeneration within ~12-13.5 h of death.[4,6] The modified technique used by Bazan's team for this study allowed for observation of new nerve structure features and, for the first time, provided a complete view of the human corneal nerve architecture. Our study reveals that aging decreases the number of central epithelial nerve terminals, and increases the presence of irregular anomalies beneath the basal layer.

Linna et al[28] have shown that corneal areas with short, unconnected nerve fiber bundles are associated with lower sensitivities than corneal areas with long nerve fiber bundles with or without interconnections. Laser-assisted *in situ* keratomileusis (LASIK)-induced alterations of subbasal nerve morphology can be visualized *via in vivo* confocal microscopy. This allows the observer to make a direct comparison of corneal sensory innervation and sensitivity to touch, pain, heat, cold, etc.

Imaging Corneal Nerves in Diabetes

These days, confocal microscopy is employed on a wide scale for studying and evaluating corneal changes in diabetic patients.[23,29-32] There are numerous reports of changes in the subbasal nerve plexus of diabetic patients due to epithelial loss and corneal hypoesthesia.[30-32] Increased light scattering due to abnormalities of the basement membrane has also been reported in a study by Morishige et al.[31,32] The importance of stromal nerve changes in diabetic patient corneas is unclear at the moment due to the lack of extensive studies using confocal microscopy. Since patients with diabetes have reduced corneal sensitivity,[30] they are more susceptible to corneal trauma. Studies by Müller et al in diabetic rats demonstrated altered morphology of corneal nerves using light and electron microscopy. In addition to the observation of polymorphism in epithelium and endothelium,[33-35] Busted et al[36] and Pierro et al[37] reported increased corneal thickness in diabetic patients.[38]

Early studies by Frueh et al[39] examined the corneas of 10 Type 1 Diabetes, 10 Type 2 Diabetes and 10 Non-diabetic patients by confocal microscopy and found epithelium and endothelium polymorphisms and abnormal stromal nerves in only two patients with Type 1 Diabetes. No specific observations on the subbasal nerves or corneal sensitivity were reported.[40] A correlation between corneal light-scattering index and stages of diabetic retinopathy was published by Morishige et al[31,32] although nerve morphology was not described. Confocal microscopy studies on skin biopsy specimens have revealed that the number of epidermal nerve fibers per unit surface area in patients with diabetic polyneuropathy is reduced.[41] Confocal microscopy appears to allow early detection of beginning neuropathy, because decreases in nerve fiber bundle counts precede impairment of corneal sensitivity.[42]

Apparently, the cornea becomes thicker in a relatively early stage of diabetes but does not further change with the degree of neuropathy. A reduction in neurotrophic stimuli in severe neuropathy may induce a thin epithelium that may lead to recurrent erosions.[30]

Corneal Nerves and Refractive Surgeries

In Photorefractive keratectomy (PRK), photoablation causes severing of the subbasal nerve plexus and anterior stromal nerves.[43,44] Tandem scanning confocal microscopy studies by Erie have shown that subbasal nerve fiber density was 98% less than pre-operatively[43] and the ablation zone center showed complete absence of branched nerve fibers, 3 months post-surgery. Both Moilanen and Erie have demonstrated that subbasal nerve density was reduced by 87%, 75% and 60%, (at 3, 6 and 12 months respectively) after PRK, and returned to preoperative levels at 2 and 3 years postoperatively.[43,45] In another study using confocal microscopy, Erie's team proved faster recovery of subbasal nerve density in the central cornea in PRK as compared to LASIK.[44] Hanneken's group have recently published an excellent review on corneal regeneration after PRK wherein they elucidate how corneal wounding develops following PRK. They also reviewed the influence of intra-operative application of mitomycin C, bandage contact lenses, anti-inflammatory and other drugs in preventing corneal haze post-PRK.[46] Laser *in situ* keratomileusis (LASIK) is a procedure that utilizes either a bladeless femtosecond laser (FS-LASIK or F-LASIK) or a traditional mechanical microkeratome (MS-LASIK) to create a corneal flap, followed by stromal ablation using an excimer laser.[47] Femtosecond laser technology was first developed in the early 1990s by Dr. Kurtz at the University of Michigan, Ann Arbor, MI, USA[48,49] and was extensively used in the surgical field of ophthalmology for its increased safety, precision and predictability over conventional microkeratomes and reduced dry eye symtoms. Femtosecond lasers emit light pulses of short duration (approximately 10-15 s) at 1053 nm wavelength that cause photodisruption of the tissue with minimum collateral damage.[48-51] This enables bladeless incisions to be performed within the tissue at various patterns and depth with high precision. A new corneal refractive procedure that does not require stromal ablation using an excimer laser called Refractive lenticule extraction (ReLEx) has been discussed by Ang et al.[52] In ReLEx, a femtosecond laser is used to create an intrastromal refractive lenticule to correct the refractive error. There are 2 versions of this. In the original ReLEx procedure, femtosecond lenticule

ISSN 2475-1278 http://dx.doi.org/10.17140/OOJ-2-108

Table 1: Mean Corneal Sensation (in millimeters) at Baseline and after the Procedures.

Reference	Number of Eyes	Age (in years)		Location of Cornea	Surgery Group	Pre-op	1W post-op	1M post-op	3M post-op	6M post-op
Wei and Wang[57]	FS-LASIK group (n=54)	25.44	±7.15 (18 to 49)	Central	FS-LASIK	5.81±0.43	2.21±1.28*	2.62±1.72*	3.79±1.44*	
					ReLEx flex	5.88±0.22	2.95±1.41**,***	3.00±1.24**	4.52±0.96**,***	
	ReLEx flex group (n=40)	24.45	±5.72 (18 to 37)		ReLEx smile	5.66±0.45	4.75±1.21**,***	5.11±1.05**,***	5.73±0.51***	
	ReLEx smile group (n=61)	27.44	±6.52 (18 to 43)	Superior	FS-LASIK	5.25±0.69	3.61±1.35*	4.09±1.35*	4.63±1.05*	
					ReLEx flex	5.21±0.85	4.43±1.16**,***	4.39±1.22**	4.98±1.03	
					ReLEx smile	5.33±0.56	4.70±0.90**,***	5.19±0.61***	5.55±0.57***	
				Inferior	FS-LASIK	5.56±0.56	2.28±1.40*	2.81±1.80*	4.19±1.32*	
					ReLEx flex	5.39±0.68	2.46±1.31**	2.93±1.37**	4.95±0.99***	
					ReLEx smile	5.66±0.47	4.92±0.79**,***	5.37±0.66**,***	5.63±0.57***	
Demirok et al[55]	F-LASIK group (n=28)	26.2	±4.4 (21 to 34)	Central	F-LASIK	56.2±5.0	30.3±15.3	31.2±14	37.5±14.8	53.7±5
					SMILE	56.8±4.7	45.6±11.5	45.3±10.5	49.3±9.9	55.9±4.9
	SMILE group (n=28)	26.2	±4.4 (21 to 34)							
				Superior	F-LASIK	54.3±4.4	34.3±12.2	35±12	41.2±10.8	53.4±4.7
					SMILE	55.3±4.6	44±9.1	44±10.2	48.7±9.5	55.3±4.9
				Inferior	F-LASIK	55.0±4.8	29.0±15	30.6±14	36.2±15	53.1±6
					SMILE	55.6±4.4	46.8±11.9	46.2±10.8	49.7±10	55.6±5.1

All values are Mean±SD standard deviation

* refers to changes of corneal sensitivity values post-op in the FS-LASIK group were significantly different from pre-op values with $p<0.05$,

** refers to changes of corneal sensitivity values post-op in the ReLEx flex group were significantly different from pre-op values with $p< 0.05$

***refers to changes of corneal sensitivity values post-op in the ReLEx flex group were significantly different from values in the FS-LASIK group with $p< 0.05$

W refers to week; M refers to month; pre-op refers to pre-surgery; post-op refers to post surgery

extraction (FLEx), mimics LASIK with the creation of an anterior hinged flap. The lenticule is peeled away after the flap is lifted. Small incision lenticule extraction (SMILE) is a refined version of ReLEx and does not need flap-creation. It involves lenticule dissection and extraction from a small curved bow-like incision (2.5-3 mm) positioned superiorly.[52,53] In a prospective, randomized clinical trial (contralateral-eye study), 28 patients with myopia or myopic astigmatism in both eyes were enrolled. One eye of each patient was treated by SMILE, and the fellow eye was treated by F-LASIK. One of the mean outcome measures for corneal sensation was Cochet-Bonnet esthesiometry[54] and patients were evaluated pre-operatively as well as 1 week, 1 month, 3 months, and 6 months after surgery. This study by Demirok et al[55] evaluated the effects of SMILE and F-LASIK on corneal sensation and dry eye parameters revealed that although the dry eye parameters were similar in both surgical groups, there was a significant decrease in corneal sensation measured using a Cochet-Bonnet corneal esthesiometer after both types of surgery with more pronounced effects after F-LASIK surgery as compared to SMILE surgery. This difference could be attributed to the fact that LASIK disrupts both the dense subbasal nerve plexus and stromal corneal nerves in the creation of the anterior stromal flap and excimer laser ablation of the cornea whereas in SMILE there is less damage to the corneal nerve since the refractive change in SMILE is not obtained by excimer laser-induced photoablation but rather by a femtosecond laser-induced refractive cut.[56] Another non-randomized clinical trial by Wei and Wang et al[57] evaluated corneal sensitivity between FS-LASIK and femtosecond lenticule extraction (ReLEx flex) or small-incision lenticule extraction (ReLEx smile) for myopic eyes. Twenty-seven subjects (54 eyes) underwent FSLASIK, 22 subjects (40 eyes) underwent ReLEx flex, and 32 subjects (61 eyes) underwent ReLEx smile surgery. Corneal sensitivity was evaluated by Cochet-Bonnet esthesiometry preoperatively as well as at 1 week and 1 and 3 months after surgery.[58] In both trials, randomized and non-randomized, better DRY Eye outcomes were observed after SMILE as compared to femtosecond LASIK (femto LASIK) and recovery to baseline corneal sensi-

ISSN 2475-1278 http://dx.doi.org/10.17140/OOJ-2-108

Table 2: Mean Corneal Nerve Morphology (from *in-vivo* confocal microscopy; IVCM) and Corneal Sensation (in centimeters) at Baseline and after the Procedures.

Reference	Number of Eyes	Age (in years)	Parameters	Surgery Group	Pre-op	6M post-op
Vestergaard et al[56]	FLEX group (n=34)	35±7 (25 to 45)	Corneal nerve morphology (n=31 patients)	FLEX	19.00±5.51	4.78 ± 3.91
			Density (mm/mm^2, mean±SD)	SMILE	17.62±5.27	8.41±7.01*
	SMILE group (n=34)	35±7 (25 to 45)				
			Number (/mm^2, mean±SD)	FLEX	80.3±25.8	32.7±22.4
				SMILE	78.3±19.4	53.8±37.5**
			Tortuosity (grade, mean±SD)	FLEX	1.65±0.54	1.51±0.62
				SMILE	1.69±0.49	1.60±0.54
			Corneal sensation (n=34 patients)	FLEX	5.87±0.20	5.49±0.45
			Cochet-Bonnet esthesiometry (cm, mean±SD)	SMILE	5.88±0.19	5.78±0.34**

All values are Mean+SD (standard deviation)
*refers to a statistically significant difference between femtosecond lenticule extraction (FLEX) and small-incision lenticule extraction (SMILE) with $p<0.05$
**refers to a statistically significant difference between femtosecond lenticule extraction (FLEX) and small-incision lenticule extraction (SMILE) with $p<0.01$
W refers to week; M refers to month; pre-op refers to pre-surgery; post-op refers to post surgery

tivity was faster with SMILE as compared to both femto-LASIK and Femtosecond Lenticule Extraction (FLEx). Other studies by Jodhbir Mehta's group[59] have also evaluated corneal nerve changes after small incision lenticule extraction (SMILE) and laser *in situ* keratomileusis (LASIK). They found that more subbasal nerves were disrupted and undergoing regeneration after LASIK as compared to the SMILE group which in comparison demonstrated greater subbasal nerve length and density and higher subbasal nerve recovery at different time-points post-surgery (Table 1 and 2).

CORNEAL NERVE RESEARCH

New advances in imaging technology and disease models (*in vitro* cell and tissue-based as well as *in vivo* transgenic animal-based models) for studying corneal nerves and reinnervation after nerve injury or disease have further enhanced our knowledge of the corneal structure and architecture of corneal nerves in normal and diseased states.[60] The thy1-YFP transgenic mouse model developed by Joshua Sanes' group[61] which exhibits yellow fluorescent nerves in the cornea has provided an amazing tool to basic and translational scientists to study corneal nerves *in vivo* and studies using this model have yielded numerous breakthroughs and publications in the field of corneal nerve injury and regeneration research.[7,62-64] These studies have highlighted neurotoxicity in the eye due to preservatives like benzalkonium chloride and augmented the move towards non-neurotoxic preservative-free eye-drops,[62] the presence of inflammatory CD11b+GR1+myeloid-derived suppressor cells which play an important role in nerve regeneration,[65] the importance of VEGF-B in stimulating peripheral nerve growth, etc.[63]

This greater clarity and continued progress in our understanding of the functional and structural alterations of nerves in normal and disease states and their correlation with clinical signs and symptoms is crucial for the further development of targeted drug therapy and treatments for debilitating corneal diseases. The window to the future appears truly bright indeed!

ACKNOWLEDGEMENTS

The author would like to thank Ruth Zelkha from the UIC Ophthalmology Core for her help with artwork and schematic representations. Supported by National Eye Institute (NEI) Core Grant EY001792 and Research to Prevent Blindness.

FINANCIAL DISCLOSURES

The author does not have any financial or proprietary interest in any material or method mentioned.

REFERENCES

1. The definition and classification of dry eye disease: Report of the Definition and Classification Subcommittee of the International Dry Eye Work Shop. *Ocul Surf*. 2007; 5: 75-92.

2. Dua HS, Faraj LA, Said DG, Gray T, Lowe J. Human corneal anatomy redefined: A novel pre-Descemet's layer (Dua's layer). *Ophthalmology*. 2013; 120(9): 1778-1785. doi: 10.1016/j.ophtha.2013.01.018

3. Dua HS, Faraj LA, Branch MJ, et al. The collagen matrix of

ISSN 2475-1278 http://dx.doi.org/10.17140/OOJ-2-108

the human trabecular meshwork is an extension of the novel pre-Descemet's layer (Dua's layer). *Br J Ophthalmol*. 2014; 95(5): 691-697. doi: 10.1136/bjophthalmol-2013-304593

4. Muller LJ, Marfurt CF, Kruse F, Tervo TM. Corneal nerves: Structure, contents and function. *Exp Eye Res*. 2003; 76(5): 521-542. doi: 10.1016/S0014-4835(03)00050-2

5. Schlemm TFW. Nerven der Cornea [In German]. *Ammon' Z Ophthalmol*. 1831; 1: 113-114.

6. Muller LJ, Vrensen GF, Pels L, Cardozo BN, Willekens B. Architecture of human corneal nerves. *Invest Ophthalmol Vis Sci*. 1997; 38(5): 985-994. Web site. http://iovs.arvojournals.org/article.aspx?articleid=2161847. Accessed December 19, 2016.

7. Yu CQ, Rosenblatt MI. Transgenic corneal neurofluorescence in mice: A new model for in vivo investigation of nerve structure and regeneration. *Invest Ophthalmol Vis Sci*. 2007; 48(4): 1535-1542. doi: 10.1167/iovs.06-1192

8. Stern ME, Beuerman RW, Fox RI, et al. The pathology of dry eye: The interaction between the ocular surface and lacrimal glands. *Cornea*. 1998; 17(6): 584-589. Web site. https://www.pubfacts.com/detail/9820935/The-pathology-of-dry-eye-the-interaction-between-the-ocular-surface-and-lacrimal-glands. Accessed December 19, 2016.

9. Marfurt CF, Cox J, Deek S, Dvorscak L. Anatomy of the human corneal innervation. *Exp Eye Res*. 2010; 90(4): 478-492. doi: 10.1016/j.exer.2009.12.010

10. Smith JA. The epidemiology of dry eye disease: Report of the epidemiology subcommittee of the international dry eye workshop (2007). *Ocul Surf*. 2007; 5(2): 93-107.

11. Schimmelpfennig B. Nerve structures in human central corneal epithelium. *Graefes Arch Clin Exp Ophthalmol*. 1982; 218(1): 14-20. doi: 10.1007/BF02134093

12. Niederer RL, Perumal D, Sherwin T, McGhee CNJ. Age-related differences in the normal human cornea: A laser scanning in vivo confocal microscopy study. *Br J Ophthalmol*. 2007; 91(9): 1165-1169. doi: 10.1136/bjo.2006.112656

13. DelMonte DW, Kim T. Anatomy and physiology of the cornea. *J Cataract Refract Surg*. 2011; 37(3): 588-598. doi: 10.1016/j.jcrs.2010.12.037

14. Faragher RG, Mulholland B, Tuft SJ, et al. Aging and the cornea. *Br J Ophthalmol*. 1997; 81: 814-817. doi: 10.1007/978-1-59745-507-7_4

15. Waring GO 3rd, Lynn MJ, Nizam A, et al. Results of the Prospective Evaluation of Radial Keratotomy (PERK) Study five years after surgery. The Perk Study Group. *Ophthalmology*. 1991; 98(8): 1164-1176. doi: 10.1016/S0161-6420(91)32156-0

16. Dutt S, Steinert RF, Raizman MB, Puliafito CA. One-year results of excimer laser photorefractive keratectomy for low to moderate myopia. *Arch Ophthalmol*. 1994; 112(11): 1427-1436. doi: 10.1001/archopht.1994.01090230041018

17. Chatterjee A, Shah SS, Doyle SJ. Effect of age on final refractive outcome for 2342 patients following photorefractive keratectomy. *Invest Ophthalmol Vis Sci*. 1996; 37: S57.

18. Marre M. On the age dependence of the healing of corneal epithelium defects [In German]. *Albrecht Von Graefes Arch Klin Exp Ophthalmol*. 1967; 173(3): 250-255.

19. Cavanagh HD, Petroll WM, Alizadeh H, He Y-G, Mc Culley JP, Jester JV. Clinical and diagnostic use of in vivo confocal microscopy in patients with corneal disease. *Ophthalmology*. 1993; 100(10): 1444-1454. doi: 10.1016/S0161-6420(93)31457-0

20. Bohnke M, Masters BR. Confocal microscopy of the cornea. *Prog Retinal Eye Res*. 1999; 18(5): 553-628.

21. Oliveira-Soto L, Efron N. Morphology of corneal nerves using confocal microscopy. *Cornea*. 2001; 20(4): 374-384.

22. Lee J-K, Ryu Y-H, Ahn J-I, Kim M-K, Lee T-S, Kim J-C. The effect of lyophilization on graft acceptance in experimental xenotransplantation using porcine cornea. *Artif Organs*. 2010; 37-45. doi: 10.1111/j.1525-1594.2009.00789.x

23. Malik RA, Kallinikos P, Abbott CA, et al. Corneal confocal microscopy: A non-invasive surrogate of nerve fibre damage and repair in diabetic patients. *Diabetologia*. 2003; 46(5): 683-688. doi: 10.1007/s00125-003-1086-8

24. Patel DV, McGhee CN. Mapping of the normal human corneal sub-Basal nerve plexus by in vivo laser scanning confocal microscopy. *Invest Ophthalmol Vis Sci*. 2005; 46(12): 4485-4488. doi: 10.1167/iovs.05-0794

25. Stachs O, Zhivov A, Kraak R, Stave J, Guthoff R. In vivo three-dimensional confocal laser scanning microscopy of the epithelial nerve structure in the human cornea. *Graefes Arch Clin Exp Ophthalmol*. 2007; 245(4): 569-575. doi: 10.1007/s00417-006-0387-2

26. Scarpa F, Zheng X, Ohashi Y, Ruggeri A. Automatic evaluation of corneal nerve tortuosity in images from in vivo confocal microscopy. *Invest Ophthalmol Vis Sci*. 2011; 16; 52(9): 6404-6408. doi: 10.1167/iovs.11-7529

27. He J, Bazan NG, Bazan HEP. Mapping the entire human corneal nerve architecture. *Experimental Eye Research*; 2010.

ISSN 2475-1278 http://dx.doi.org/10.17140/OOJ-2-108

28. Linna TU, Vesaluoma MH, Perez-Santonja JJ, Petroll WM, Alio JL, Tervo TMT. Effect of Myopic LASIK on Corneal Sensitivity and Morphology of Subbasal Nerves. *Invest Ophthalmol Vis Sci*. 2000; 41(2): 393-439. Web site. http://iovs.arvojournals.org/article.aspx?articleid=2199874. Accessed December 19, 2016.

29. Mocan MC, Durukan I, Irkec M, Orhan M. Morphologic Alterations of Both the Stromal and Subbasal Nerves in the Corneas of Patients with Diabetes. *Cornea*. 2006; 25(7): 769-773. doi: 10.1097/01.ico.0000224640.58848.54

30. Rosenberg ME, Tervo TM, Immonen IJ, et al. Corneal structure and sensitivity in type 1 diabetes mellitus. *Invest Ophthalmol Vis Sci*. 2000; 41(10): 2915-2921. Web site. http://iovs.arvojournals.org/article.aspx?articleid=2123743. Accessed December 19, 2016.

31. Morishige N, Chikama T, Sassa Y, Nishida T. Correlation of corneal light scattering index measured by a confocal microscope with stages of diabetic retinopathy [ARVO Abstract]. *Invest Ophthal Mol Vis Sci*. 1999; 40(4): S620.

32. Morishige N, Chikama TI, Sassa Y, et al. Abnormal light scattering detected by confocal biomicroscopy at the corneal epithelial basement membrane of subjects with type II diabetes. *Diabetologia*. 2001; 44(3): 340-345. doi: 10.1007/s001250051624

33. Ruben ST. Corneal sensation in insulin dependent and non-insulin dependent diabetics with proliferative retinopathy. *Acta Ophthal Mol*. 1994; 72(5): 576-580. doi: 10.1111/j.1755-3768.1994.tb07182.x

34. Schultz RO, Matsuda M, Yee RW, Edelhauser HF, Schultz KJ. Corneal endothelial changes in type I and type II diabetes mellitus. *Am J Ophthalmol*. 1984; 98(4): 401-410. doi: 10.1111/aos.12064

35. Schultz RO, Peters MA, Sobocinski K, Nassif K, Schultz KJ. Diabetic corneal neuropathy. *Trans Am Ophthalmol Soc*. 1983; 81: 107-124.

36. Busted N, Olsen T, Schmitz O. Clinical observations on the corneal thickness and the corneal endothelium in diabetes mellitus. *Br J Ophthalmol*. 1981; 65(10): 687-690. doi: 10.1136/bjo.65.10.687

37. Pierro L, Brancato R, Zaganelli E. Correlation of corneal thickness with blood glucose control in diabetes mellitus. *Acta Ophthalmol*. 1993; 71(2): 169-172. doi: 10.1111/j.1755-3768.1993.tb04984.x

38. McNamara NA, Brand RJ, Polse KA, Bourne WM. Corneal function during normal and high serum glucose levels in diabetes. *Invest Ophthalmol Vis Sci*. 1998; 39(1): 3-17. Web site. http://iovs.arvojournals.org/article.aspx?articleid=2180804. Accessed December 19, 2016.

39. Frueh BE, Ko¨rner U, Bo¨hnke M. Konfokale Mikroskopie der Horn- haut bei Patienten mit Diabetes mellitus [In German]. *Klin Monatsbl Augen-Heilkd*. 1995; 206(5): 317-319. doi: 10.1055/s-2008-1035450

40. Ishida N, Rao GN, del Gerro M, Aquavella JV. Corneal nerve alterations in diabetes mellitus. *Arch Ophthalmol*. 1984; 102(9): 1380-1384. doi: 10.1001/archopht.1984.01040031122038

41. Kennedy WR, Wendelschafer-Crabb G, Johnson T. Quantitation of epidermal nerves in diabetic neuropathy. *Neurology*. 1996; 47(4): 1042-1048. doi: 10.1212/WNL.47.4.1042

42. Nielsen NV, Lund FS. Diabetic polyneuropathy: Corneal sensitivity, vibratory perception and Achilles tendon reflex in diabetics. *Acta Neurol Scand*. 1979; 59(1): 15-22. doi: 10.1111/j.1600-0404.1979.tb02906.x

43. Erie JC. Corneal wound healing after photorefractive keratectomy: A 3-year confocal microscopy study. *Trans Am Ophthalmol Soc*. 2003; 101: 293-333.

44. Erie JC, McLaren JW, Hodge DO, Bourne WM. Recovery of corneal subbasal nerve density after PRK and LASIK. *Am J Ophthalmol*. 2005; 140(6): 1059-1064. doi: 10.1016/j.ajo.2005.07.027

45. Moilanen JA, Vesaluoma MH, Müller LJ, Tervo TM. Long-term corneal morphology after PRK by in vivo confocal microscopy. *Invest Ophthalmol Vis Sci*. 2003; 44(3): 1064-1069. doi: 10.1167/iovs.02-0247

46. Juan JT, Larranasga AMG, Hanneken L. Corneal regeneration after photorefractive keratectomy: A review. *J Optom*. 2015; 8(3): 149-169. doi: 10.1016/j.optom.2014.09.001

47. Shortt AJ, Allan BD. Photorefractive keratectomy (PRK) versus laser-assisted in-situ keratomileusis (LASIK) for myopia. *Cochrane Database Syst Rev*. 2006; 19: CD005135. doi: 10.1002/14651858.CD005135.pub2

48. Aristeidou A, Taniguchi EV, Tsatsos M, et al. The evolution of corneal and refractive surgery with the femtosecond laser: A review. *Eye and Vision*. 2015; 2: 12. doi: 10.1186/s40662-015-0022-6

49. Soong HK, Malta JB. Femtosecond lasers in ophthalmology. *Am J Ophthalmol*. 2009; 147: 189-197.

50. Stern D, Schoenlein RW, Puliafito CA, Dobi ET, Birngruber R, Fujimoto JG. Corneal ablation by nanosecond, picosecond, and femtosecond lasers at 532 and 625 nm. *Arch Ophthalmol*. 1989; 107(4): 587-592. doi: 10.1001/archopht.1989.01070010601038

ISSN 2475-1278 http://dx.doi.org/10.17140/OOJ-2-108

51. Ratkay-Traub I, Ferincz IE, Juhasz T, Kurtz RM, Krueger RR. First clinical results with the femtosecond neodymium-glass laser in refractive surgery. *J Refract Surg*. 2003; 19(2): 94-103. doi: 10.3928/1081-597X-20030301-03

52. Ang M, Chaurasia SS, Angunawela RI, et al. Femtosecond lenticule extraction (FLEx): Clinical results, interface evaluation, and intraocular pressure variation. *Invest Ophthalmol Vis Sci*. 2012; 53: 1414-1421. doi: 10.1167/iovs.11-8808

53. Sekundo W, Kunert KS, Blum M. Small incision corneal refractive surgery using the small incision lenticule extraction (SMILE) procedure for the correction of myopia and myopic astigmatism: Results of a 6 month prospective study. *Br J Ophthalmol*. 2011; 95(3): 335-339. doi: 10.1136/bjo.2009.174284

54. Beuerman RW, McCulley JP. Comparative clinical assessment of corneal sensation with a new aesthesiometer. *Am J Ophthalmol*. 1978; 86(6): 812-815. doi: 10.1016/0002-9394(78)90127-7

55. Demirok A, Ozgurhan EB, Agca A, et al. Corneal sensation after corneal refractive surgery with small incision lenticule extraction. *Optom Vis Sci*. 2013; 90(10): 1040-1047. doi: 10.1097/OPX.0b013e31829d9926

56. Vestergaard AH, Grønbech KT, Grauslund J, Ivarsen AR, Hjortdal JØ. Subbasal nerve morphology, corneal sensation, and tear film evaluation after refractive femtosecond laser lenticule extraction. *Graefes Arch Clin Exp Ophthalmol*. 2013; 251(11): 2591-2600. doi: 10.1007/s00417-013-2400-x

57. Wei S, Wang Y. Comparison of corneal sensitivity between FS-LASIK and femtosecond lenticule extraction (ReLEx flex) or small-incision lenticule extraction (ReLEx smile) for myopic eyes. *Graefes Arch Clin Exp Ophthalmol*. 2013; 251(6): 1645-1654. doi: 10.1007/s00417-013-2272-0

58. Tsubota K, Chiba K, Shimazaki J. Corneal epithelium in diabetic patients. *Cornea*. 1991; 10(2): 156-160.

59. Mohamed-Noriega K, Riau AK, Lwin NC, Chaurasia SS, Tan DT, Mehta JS. Early corneal nerve damage and recovery following small incision lenticule extraction (SMILE) and laser in situ keratomileusis (LASIK). *Invest Ophthalmol Vis Sci*. 2014; 55(3): 1823-1834. doi: 10.1167/iovs.13-13324

60. Shaheen BS, Bakir M, Jain S. Corneal nerves in health and disease. *Surv Ophthalmol*. 2014; 59(3): 263-285. doi: 10.1016/j.survophthal.2013.09.002

61. Feng G, Mellor RH, Bernstein M, et al. Imaging neuronal subsets in transgenic mice expressing multiple spectral variants of GFP. *Neuron*. 2000; 28(1): 41-51. doi: 10.1016/S0896-6273(00)00084-2

62. Sarkar J, Chaudhary S, Namavari A, et al. Corneal neurotoxicity due to topical benzalkonium chloride. *Invest Ophthalmol Vis Sci*. 2012; 53(4): 1792-1802. doi: 10.1167/iovs.11-8775

63. Guaiquil VH, Pan Z, Karagianni N, Fukuoka S, Alegre G, Rosenblatt MI. VEGF-B selectively regenerates injured peripheral neurons and restores sensory and trophic functions. *Proc Natl Acad Sci USA*. 2014; 111(48): 17272-17277. doi: 10.1073/pnas.1407227111

64. Namavari A, Chaudhary S, Sarkar J, et al. In vivo serial imaging of regenerating corneal nerves after surgical transection in transgenic thy1-YFP mice. *Invest Ophthalmol Vis Sci*. 2011; 52(11): 8025-8032. doi: 10.1167/iovs.11-8332

65. Sarkar J, Chaudhary S, Jassim SH, et al. CD11b+GR1+ myeloid cells secrete NGF and promote trigeminal ganglion neurite growth: Implications for corneal nerve regeneration. *Invest Ophthalmol Vis Sci*. 2013; 54(9): 5920-5936. doi: 10.1167/iovs.13-12237